



**Single point power Intel[®] Model: 18260NGW, FCC
ID: PD918260NG**

Intel model 18260NGW embedded inside Lenovo model TP00078A

RF Exposure Power Density and Evaluation Test Report

July 2016

Revision 1.5



Notice: This document contains information on products in the design phase of development. The information here is subject to change without notice. Do not finalize a design with this information.

INFORMATION IN THIS DOCUMENT IS PROVIDED IN CONNECTION WITH INTEL PRODUCTS. NO LICENSE, EXPRESS OR IMPLIED, BY ESTOPPEL OR OTHERWISE, TO ANY INTELLECTUAL PROPERTY RIGHTS IS GRANTED BY THIS DOCUMENT. EXCEPT AS PROVIDED IN INTEL'S TERMS AND CONDITIONS OF SALE FOR SUCH PRODUCTS, INTEL ASSUMES NO LIABILITY WHATSOEVER AND INTEL DISCLAIMS ANY EXPRESS OR IMPLIED WARRANTY, RELATING TO SALE AND/OR USE OF INTEL PRODUCTS INCLUDING LIABILITY OR WARRANTIES RELATING TO FITNESS FOR A PARTICULAR PURPOSE, MERCHANTABILITY, OR INFRINGEMENT OF ANY PATENT, COPYRIGHT OR OTHER INTELLECTUAL PROPERTY RIGHT.

A "Mission Critical Application" is any application in which failure of the Intel Product could result, directly or indirectly, in personal injury or death. SHOULD YOU PURCHASE OR USE INTEL'S PRODUCTS FOR ANY SUCH MISSION CRITICAL APPLICATION, YOU SHALL INDEMNIFY AND HOLD INTEL AND ITS SUBSIDIARIES, SUBCONTRACTORS AND AFFILIATES, AND THE DIRECTORS, OFFICERS, AND EMPLOYEES OF EACH, HARMLESS AGAINST ALL CLAIMS COSTS, DAMAGES, AND EXPENSES AND REASONABLE ATTORNEYS' FEES ARISING OUT OF, DIRECTLY OR INDIRECTLY, ANY CLAIM OF PRODUCT LIABILITY, PERSONAL INJURY, OR DEATH ARISING IN ANY WAY OUT OF SUCH MISSION CRITICAL APPLICATION, WHETHER OR NOT INTEL OR ITS SUBCONTRACTOR WAS NEGLIGENT IN THE DESIGN, MANUFACTURE, OR WARNING OF THE INTEL PRODUCT OR ANY OF ITS PARTS.

Intel may make changes to specifications and product descriptions at any time, without notice. Designers must not rely on the absence or characteristics of any features or instructions marked "reserved" or "undefined." Intel reserves these for future definition and shall have no responsibility whatsoever for conflicts or incompatibilities arising from future changes to them. The information here is subject to change without notice. Do not finalize a design with this information.

Intel software products are copyrighted by and shall remain the property of Intel Corporation. Use, duplication, or disclosure is subject to restrictions stated in Intel's Software License Agreement, or in the case of software delivered to the government, in accordance with the software license agreement as defined in FAR 52.227-7013.

The products described in this document may contain design defects or errors known as errata which may cause the product to deviate from published specifications. Current characterized errata are available on request.

The code names presented in this document are only for use by Intel to identify products, technologies, or services in development that have not been made commercially available to the public, i.e., announced, launched, or shipped. They are not "commercial" names for products or services and are not intended to function as trademarks.

Contact your local Intel sales office or your distributor to obtain the latest specifications and before placing your product order.

Copies of documents which have an order number and are referenced in this document, or other Intel literature may be obtained by calling 1-800-548-4725 or by visiting Intel's website at <http://www.intel.com/design/literature.htm>.

Intel processor numbers are not a measure of performance. Processor numbers differentiate features within each processor family, not across different processor families. See http://www.intel.com/products/processor_number for details.

Intel is a trademark of Intel Corporation or in the US and other countries.

* Other brands and names may be claimed as the property of others.

Copyright © 2015 Intel Corporation. All rights reserved.



Contents

1	Document Scope	7
2	Background – WiGig System Operation	8
2.1	System block diagram	8
2.2	Beam forming	9
2.3	TX duty cycle	9
2.4	Intel 18260NGW module in Lenovo model TP00078A	9
3	Simulation Methodology	10
3.1	Assessment method	10
3.2	Near field & transition-zone field results	10
3.3	Simulation tool	10
3.3.1	Solver description	10
3.3.2	Tool description	10
3.3.3	Convergence criteria and Power Density Calculations	11
3.4	Finding near field worst case simulation configuration	11
3.4.1	Terminology:	12
3.4.2	Primer on field vector representation:	13
3.4.3	Domain search for worst case direction	15
3.5	Worst case operating conditions of the platform	17
3.6	3D models used in the simulation	18
3.6.1	RFEM 2 housing inside Intel 18260NGW module	18
3.6.2	Antenna distance to the body of an end user	19
3.6.3	Metals in proximity of the RFEM 2	20
3.7	Antenna feed	21
4	Simulation Results	22
4.1	Results on the edge area.	23
4.1.1	Upper bound simulation results	23
4.1.2	Single-point power density values with worst-case antenna phases for edge plane exposure	27
4.1.3	One dimensional cut of the mesh single-point power density for edge plane exposure	31
4.1.4	Integrated power density over 1 cm ² for edge plane exposure	32
4.1.5	Power density	34
4.2	Results on the base area	35
4.2.1	Upper bound simulation results	35
4.2.2	Single-point power density values with worst antenna phases for base plane exposure	38
4.2.3	One dimensional cut of the mesh single-point power density for base plane exposure	42
4.2.4	Integrated power density over 1 cm ² for base plane exposure	43
4.2.5	Power density	46
4.3	Conclusion	48
5	Validation of Simulation Model in transition-zone Field to Far-Field	49
5.1	Correlation of power density in far field	49
5.1.1	Far field boundary calculation	49
5.1.2	Laboratory Test	50
5.1.3	Correlation of measurements and simulation	50
5.1.4	Estimating conducted power level	53
5.2	Simulating a canonical antenna design	54
6	Summary	57



List of Figures

FIGURE 1 – INTEL 18260NGW MODULE SYSTEM BLOCK DIAGRAM	8
FIGURE 2 – ILLUSTRATION OF THE ADAPTIVE MESH TECHNIQUE	11
FIGURE 3 – SEARCH PLANES ARE THE X-Y PLANES (I.E. THE TRANSPARENT PLANE AS ILLUSTRATED IN THIS PICTURE- LEFT: EDGE PLANE RIGHT: BASE PLANE)	12
FIGURE 4 – NEAR FIELD WORST CASE TERMINOLOGY AND ORIENTATION	12
FIGURE 5 – PLATFORM OPERATING MODES.....	17
FIGURE 6 - PLATFORM WORST CASE OPERATING MODE	17
FIGURE 7– ACTIVE ANTENNA INSIDE THE PLATFORM	18
FIGURE 8 - SIMULATED AREA ON THE BASE	19
FIGURE 9 - SIMULATED AREA ON THE EDGE.....	20
FIGURE 10 – EDGE PLANE ILLUSTRATION	23
FIGURE 11 – CHANNEL 1 UPPER BOUND, SINGLE-POINT POWER DENSITY MESH ON PLATFORM EDGE AT 100% DUTY CYCLE	24
FIGURE 12 – CHANNEL 2 UPPER BOUND, SINGLE-POINT POWER DENSITY MESH ON PLATFORM EDGE AT 100% DUTY CYCLE	24
FIGURE 13 – CHANNEL 3 UPPER BOUND, SINGLE-POINT POWER DENSITY MESH ON PLATFORM EDGE AT 100% DUTY CYCLE	25
FIGURE 14 – FOOTPRINT IN EDGE PLANE.....	26
FIGURE 15 – CHANNEL 1 SINGLE-POINT POWER DENSITY MESH ON PLATFORM EDGE	29
FIGURE 16 – CHANNEL 2 SINGLE-POINT POWER DENSITY MESH ON PLATFORM EDGE	29
FIGURE 17 – CHANNEL 3 SINGLE-POINT POWER DENSITY MESH ON PLATFORM EDGE	30
FIGURE 18 - ONE DIMENSIONAL PLOTS OF THE POWER DENSITY ON CHANNEL 1	31
FIGURE 19 - ONE DIMENSIONAL PLOTS OF THE POWER DENSITY ON CHANNEL 2	31
FIGURE 20 - ONE DIMENSIONAL PLOTS OF THE POWER DENSITY ON CHANNEL 3	31
FIGURE 21 – CHANNEL 1 WORST CASE - INTEGRATED POWER OVER 1CM ² AN PLATFORM EDGE.....	32
FIGURE 22 – CHANNEL 2 WORST CASE - INTEGRATED POWER OVER 1CM ² AN PLATFORM EDGE.....	32
FIGURE 23 – CHANNEL 3 WORST CASE - INTEGRATED POWER OVER 1CM ² AN PLATFORM EDGE.....	33
FIGURE 24 – ELEVATION AND AZIMUTH ANGLES.....	35
FIGURE 25 – CHANNEL 1 UPPER BOUND, SINGLE-POINT POWER DENSITY MESH ON PLATFORM BASE AT 100% DUTY CYCLE	36
FIGURE 26 – CHANNEL 2 UPPER BOUND, SINGLE-POINT POWER DENSITY MESH ON PLATFORM BASE AT 100% DUTY CYCLE	36
FIGURE 27 – CHANNEL 3 UPPER BOUND, SINGLE-POINT POWER DENSITY MESH ON PLATFORM BASE AT 100% DUTY CYCLE	37
FIGURE 28 – CHANNEL 1 SINGLE-POINT POWER DENSITY MESH ON PLATFORM BASE	40
FIGURE 29 – CHANNEL 2 SINGLE-POINT POWER DENSITY MESH ON PLATFORM BASE	40
FIGURE 30 – CHANNEL 3 SINGLE-POINT POWER DENSITY MESH ON PLATFORM BASE	41
FIGURE 31 - ONE DIMENSIONAL PLOTS OF THE POWER DENSITY ON CHANNEL 1	42
FIGURE 32 - ONE DIMENSIONAL PLOTS OF THE POWER DENSITY ON CHANNEL 2	42
FIGURE 33 - ONE DIMENSIONAL PLOTS OF THE POWER DENSITY ON CHANNEL 3	42
FIGURE 34 – CHANNEL 1 WORST CASE - INTEGRATED POWER OVER 1CM ² AN PLATFORM BASE	43
FIGURE 35 – CHANNEL 2 WORST CASE - INTEGRATED POWER OVER 1CM ² AN PLATFORM BASE	44
FIGURE 36 – CHANNEL 3 WORST CASE - INTEGRATED POWER OVER 1CM ² AN PLATFORM EDGE.....	45
FIGURE 37 – HFSS SIMULATION RESULTS IN CHANNEL 1	46
FIGURE 38 – HFSS SIMULATION RESULTS IN CHANNEL 2	47
FIGURE 39 – HFSS SIMULATION RESULTS IN CHANNEL 3	47
FIGURE 40 – ANTENNA DIMENSIONS.....	49
FIGURE 41 - COMPARISON OF E.I.R.P. SIMULATION RESULTS TO LAB MEASUREMENTS – CHANNEL 1	50
FIGURE 42 - COMPARISON OF E.I.R.P. SIMULATION RESULTS TO LAB MEASUREMENTS – CHANNEL 2	51
FIGURE 43 - COMPARISON OF E.I.R.P. SIMULATION RESULTS TO LAB MEASUREMENTS – CHANNEL 3	51
FIGURE 44 - ESTIMATE CONDUCTED POWER FROM EIRP DATA	53
FIGURE 45 - SIMULATION OF A SINGLE PATCH ANTENNA	54
FIGURE 46 – PATCH ANTENNA GAIN	54
FIGURE 47 – SIMULATION 3D STRUCTURE	55
FIGURE 48– POWER DENSITY OF CANONICAL PATCH ANTENNA	56



List of Tables

TABLE 1 – ACRONYMS 5
 TABLE 2 - PHASES CONFIGURATIONS FOR THE WORST CASE..... 27
 TABLE 3 – RATIOS BETWEEN Z-POWER DENSITY AND TOTAL POWER DENSITY ON EDGE AREA 28
 TABLE 4 - WORST CASE POWER DENSITY - EDGE PLANE 34
 TABLE 5 –EDGE PLANE INTEGRATED POWER DENSITY AT ZERO DISTANCE 34
 TABLE 6 - PHASES CONFIGURATIONS FOR THE WORST CASE..... 38
 TABLE 7 – RATIOS BETWEEN Z-POWER DENSITY AND TOTAL POWER DENSITY ON BASE AREA 39
 TABLE 8 –BASE PLANE INTEGRATED POWER DENSITY AT ZERO DISTANCE 48
 TABLE 9 – GAIN CALCULATION FROM POWER DENSITY PER SEVERAL DISTANCES 55
 TABLE 10 – SUMMARY OF SIMULATION RESULTS FOR RF EXPOSURE COMPLIANCE..... 57

Table 1 – Acronyms

ABS	Acrylonitrile butadiene styrene – the plastic type from which the Lenovo model TP00078A is built
Ant	Antenna
Az	Azimuth
BB	Base Band
BF	Beam Forming
BT	Bluetooth
BW	Band Width
CAD	Computer Aided Design
CPU	Central Processing Unit
EIRP	Equivalent Isotropically Radiated Power
EI	Elevation
EM	Electro-Magnetic
GHz	Giga Hertz (10 ⁹ Hz)
IF	Intermediate Frequency
MAC	Media Access Control
M.2	Formerly known as Next Generation Form Factor (NGFF); used as specification for connectors of the expansions cards mounted on computer.
mmWave	Milli-Meter Wave
OTP	One Time Programmable memory



PC	Personal Computer
R&D	Research and Development
RF	Radio Frequency
RFEM	Radio Front End Module
RFIC	Radio Frequency Integrated Circuit
RX	Receive
SKU	Stock Keeping Unit, specific product model version
TPC	Transmit Power Control
T/R SW	Transmit / Receive Switch
TX	Transmit
WiGig	Wireless Gigabit Alliance – the alliance that promoted the 60GHz into 802.11ad standard.



1 Document Scope

This report is submitted to support the compliance to FCC rule parts §2.1093 and §15.255(g), of Intel 18260NGW WiGig module (FCC ID: PD918260NG), including an active antenna array, embedded inside the Lenovo Model TP00078A platform.

Please note, Lenovo model TP00078A is the regulatory model number. This identical host is also marketed under the name Lenovo ThinkPad Yoga 260. In the report we refer only to TP00078A model.

Per the location of the active antenna array (a.k.a. RFEM 2) in the Lenovo model TP00078A platform, the distance between the antenna array to the body of an end user, at the closest contact point, will be in the near field. At this time power density measurements are not possible.

Therefore, to obtain an estimation of the near field power density results, we used an EM simulation that includes the RFEM 2 transmitter model, embedded inside the Lenovo model TP00078A. The simulation method and the simulation results are described in this document.

Due to the lack of standardized code validation, benchmarking and uncertainty of the simulation software, the near field ¹to far field results are included for the purpose of providing confidence for the software simulation model used and that the results produced were within an acceptable range when compared with the measured results. The error margins of all test results have been considered collectively by the FCC to determine compliance.

To prove the validity of these results, this report shows how the results of the same simulation are correlated to lab measurements for transition-zone ² field to far field distances.

The 2nd chapter provides relevant background on Intel 18260NGW module. The 3rd chapter describes the simulation methodology to determine RF exposure (power density) levels. The 4th chapter includes simulation results, and 5th chapter the correlation between simulation and lab measurements in transition-zone field to far field^{3,4}. Chapter 6 summarizes the RF-Exposure analysis.

Please note that this document covers non confidential parts information, relevant details and explanations that qualify for confidentiality are included separately in the Operational Descriptions document/exhibit; therefore, not included in the this reports. However, in this document some places make cross-reference to the confidential Operational Description exhibit for details about device operation.

¹ The "near field" nomination is used to indicate the reactive near field zone at antenna proximity particularly the field in the exposure plane. In this report it is the zone between 0 and 5 cm.

² The transition-zone field nomination is used to indicate the radiative near field zone in which the correlation between the measurement and simulation is performed i.e, it is the zone between 5cm and 10 cm

³ The Far field zone nomination is used to indicate the zone above 10cm from the antenna.

⁴ The far field lower distance (10 cm) is determined according to the RFEM 2 dimension. The transition-zone field is the zone going from the lower limit of the measurement distance (5 cm) to the far field lower limit (10 cm).

2 Background – WiGig System Operation

2.1 System block diagram

Intel 18260NGW module (FCC ID: PD918260NG) is a solution for embedded WiGig connectivity for various PC client platforms. For this RF exposure evaluation the Intel 18260NGW module will be incorporated into the Lenovo model TP00078A PC. The Lenovo TP00078A is a 2 in 1 PC that can be used in traditional portable laptop notebook mode or converted to a tablet PC (non-detachable) mode.

The client solution for Lenovo TP00078A includes the 18260NGW WiGig module (FCC ID: PD918265NG) connected to a beamforming antenna array RFEM 2 using one IF coax cable.

The WiGig module (FCC ID: PD918265NG) is a PCIe M.2 module consisting of a WiGig BB chip, which implements the WiGig MAC, Modem, BF algorithm, and active antenna array module control, as well as the BB + IF stage circuitry. This WiGig module re-uses the same WiGig MAC/BB silicon core as the previous generation module 17260NGW (FCC ID: PD917260NG).

RFEM 2 (10042RRFW) is an active antenna array module, which converts the IF signal to 60GHz signal. It also performs the beamforming functionality by phase shifting the RF signal that goes to each antenna. The RFEM 2 is slave to the WiGig BB chip since all module control and algorithms run on the BB chip.

Intel System-on-Chip (SoC) houses the CPU (central processing unit) which executes different applications, as well as provides the command and control of the client solution, including all I/O data and addressing.

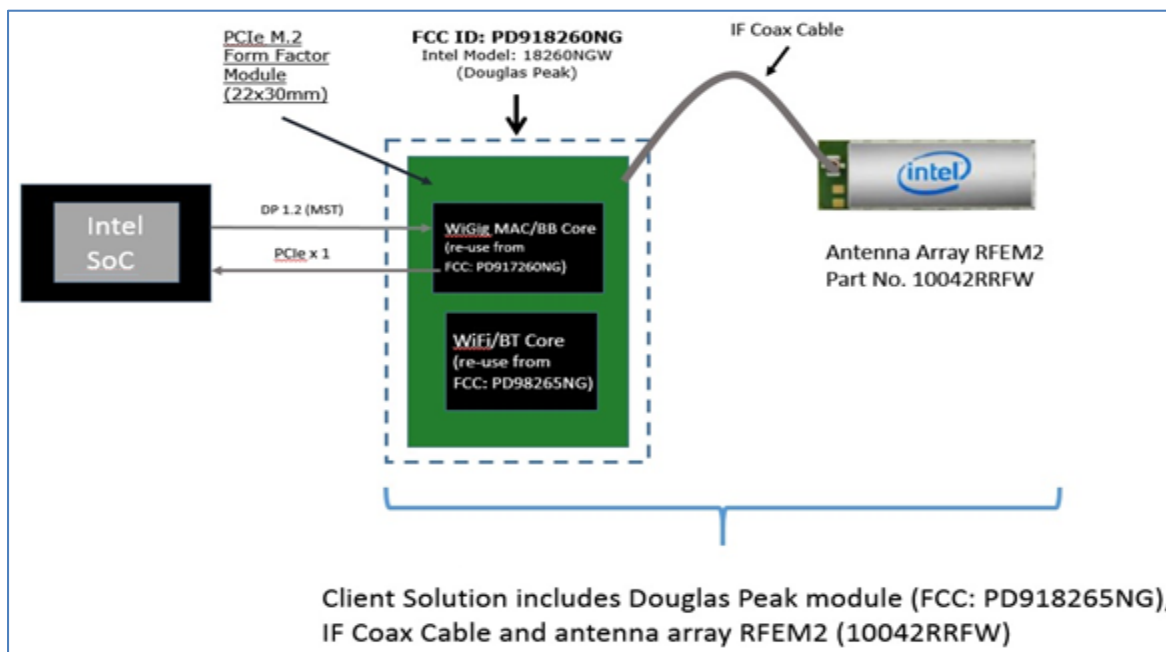


Figure 1 – Intel 18260NGW module system block diagram

In typical application the RFEM 2 is located at the top of the lid of the platform, in order to improve the RF propagation of the communication link



2.2 Beam forming

Achieving high bandwidth communication over 60GHz channels usually requires directional antenna at the transmitter and receiver sides. In consumer electronics, fixed directional or mechanically rotated antenna are not practical and electronically steerable antenna are usually used.

In Intel 18260NGW module, such electronic steerable antenna array is being used. Beam forming protocol (defined in the standard ISO/IEC/IEEE 8802-11:2012/Amd.3:2014(E), Clause 21 is used to find the right direction for setting both the RX and TX antenna directions.

Due to the RFEM 2 structure it is not easy to predict the direction and beam forming combination that yields the maximum energy in near field. To find this value a search over the possible beam forming combination was made and the worst case value was taken. Detailed explanation of this process can be found in section 3.4.

2.3 TX duty cycle

The WiGig protocol, as defined in ISO/IEC/IEEE 8802-11:2012/Amd.3:2014(E), Clause 21, is packet based with time division multiplexing (TDM). Intel 18260NGW module is configured to guarantee that the TX-Duty-Cycle, defined as the ratio of the duration of all transmissions to the total time, is at most 70% over any 10 seconds period. This was established by worst case analysis, as derived from full system simulation, and verified by measurements.

The limited TX-Duty-Cycle is established based on HW and FW implementation with ~100 ms (102.4 ms) measurement duration and 10 seconds averaging; other details are provided in the Operational Description exhibit. The 70% duty cycle limitation is guaranteed independent of user activity, and therefore it adheres to the source-based time-averaging definition in 2.1093(d)(5).

In addition, measurements of the Intel 18260NGW module configured to obtain maximal TX-Duty-Cycle in a fully loaded system, resulted in actual maximum TX-Duty-Cycle of 58% over any 10 seconds period, lower than the upper bound derived from the analysis in this section.

2.4 Intel 18260NGW module in Lenovo model TP00078A

Intel produces several HW SKUs (variations) of Intel 18260NGW module, which target different types of customer platform products.

Lenovo uses Intel 18260NGW module inside the Lenovo Model TP00078A platform. This SKU is characterized by:

- supporting channels **1+2+3**
- Reduced power emission, which translates to:
 - a. Maximum transmit conducted power of **6.6 dBm** aggregated conducted power at the antenna ports.
 - b. Maximum TX duty-cycle of **70%**.
- Antenna array RFEM 2 (100042RRFW).

- Note that antenna array RFEM 2 (100041RRFW) was also approved as part of the module original approval but is not being implemented with the Lenovo TP00078A. No other antennas have been approved by original or permissive change filings.



3 Simulation Methodology

3.1 Assessment method

During system operation mode it is challenging to define practical system worst case scenario in which the user is exposed to highest emission level. To ensure coverage of the highest emission the analysis of the worst case corner condition is used and is emphasized in the following:

1. Platform orientation with respect to human body – in most of the cases when the platform is very close to the human body and the energy is directed to the human body, the human body will attenuate the signal. In this case a reliable link can't be achieved, when a reliable link can't be maintained the system enters search mode. In search mode the system will transmit a low duty cycle of less than 1%. This search mode contains signals which happen every 100ms at the maximum output power.
However – in the analysis done in this document system is simulated in operational mode (not in search mode) operating at 70% duty cycle which is much higher than the search mode.
2. Energy direction, beam forming – In order to avoid human body attenuation or object blockage of a reliable link the system beam forming will automatically search for a path that will establish a more reliable link. So, in real life, in most of the cases the EM path will not be directed towards the human body.
However – in the analysis presented in this document worst case beam forming direction is used.

Please note; the above worst case assessment description is very conservative in that it is very unlikely this case would happen under normal usage conditions. Since we cannot state with 100% certainty that this is impossible we kept this worst case assessment methodology, we ask that this is taken into consideration.

3.2 Near field & transition-zone field results

Finding the worst case emission in near field across platform boundary requires searching on two orthogonal domains. One domain is the location – need to find the place that has the worst case energy. The other domain that has to be searched is the antenna phases – need to search over the various antenna phases and find the antenna phase combination that gives the worst case value. Section 3.4 below explains how these two worst case phase searches are investigated.

After the completion of the worst case phase analysis, the phases found during this analysis are used to find the worst case integrated energy across 1cm² averaging area for RF exposure evaluation purposes. EM simulation is used for this analysis.

Transition-zone field to far field analysis is both simulated and correlated against measured lab results.

3.3 Simulation tool

3.3.1 Solver description

The HFSS simulation is done using the Finite Element Method which operates in the frequency domain. The HFSS is based on an accurate direct solver with first order basis functions.

3.3.2 Tool description

For the EM simulation the commercial ANSYS Electronics Desktop 2015 (HFSS) is used. The ANSYS HFSS tool is used in industry for simulating 3-D full-wave electromagnetic fields. Intel uses this EM simulation tool due to its' gold-standard accuracy, advanced solver and high-performance computing technology capabilities for doing accurate and rapid design of high-frequency components.

3.3.3 Convergence criteria and Power Density Calculations

The HFSS uses volume air box containing the simulated area to calculate the EM fields. The box is truncated by PML (Perfect Match Layer) boundary condition. The simulation uses adaptive mesh technique (see below Figure 2) to meet the exit criteria of $\Delta S < 0.02$. The delta S is the change in the magnitude of the S-parameters between two consecutive passes, if the magnitude and phase of all S-parameters change by an amount less than the Maximum Delta S per Pass value from one iteration to the next, the adaptive analysis stops.

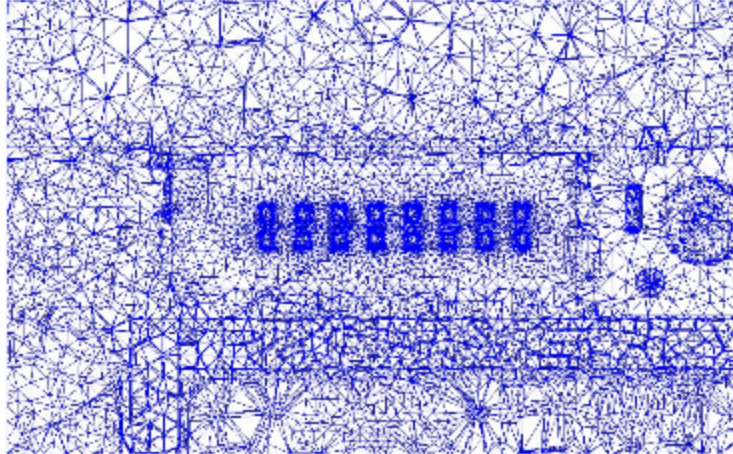


Figure 2 – Illustration of the Adaptive Mesh Technique

After having the simulated electrical and magnetic (E & H) fields in each point in the mesh, the Poynting vector is calculated. The integrated power density on a given surface is calculated as the surface integral of the Poynting vector:

$$W = \frac{1}{2} \text{Re} \int_S (\vec{E} \times \vec{H}^*) \cdot \vec{n} dS$$

Note: HFSS phasors in field calculator are peak phasors which leads to the $\frac{1}{2}$ factor in the Poynting vector calculation.

3.4 Finding near field worst case simulation configuration

As explained previously near field analysis requires finding worst case location (along the searched planes) and antenna phase values. As further explained the search should be done on two domains:

- 1) Look for the worst case position (across the search plane).
- 2) Look for the worst case antenna phases

Note: the search plane here is defined as the plane that is used for the calculation of the worst case antenna phase values.

The two x-y planes below represent the worst case scenarios where the user is the closest to the platform:

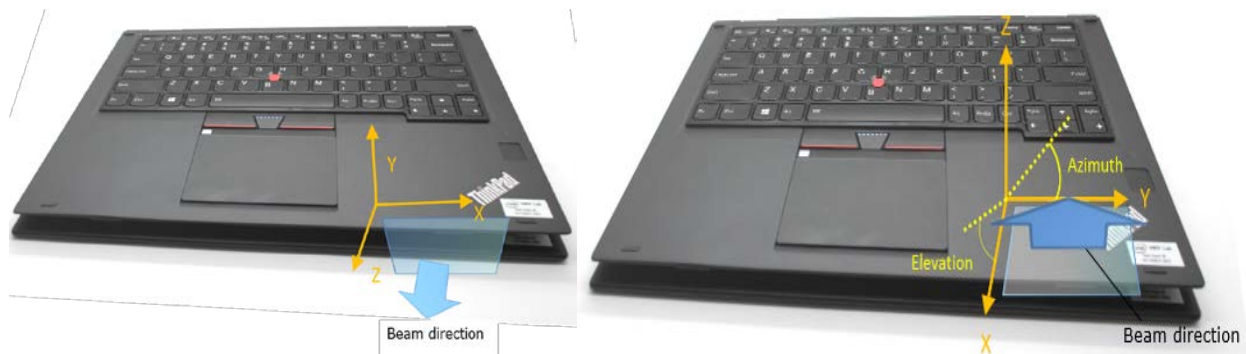


Figure 3 – Search Planes are the x-y planes (i.e. the transparent plane as illustrated in this picture- Left: Edge plane Right: Base plane)

Note that for xyz coordinate reference used in this report, we always consider the z-axis towards the body direction. This explains the fact that the axis convention is different between the edge and the base planes. This consideration is used to conserve a general consistency for the fields representation and calculations in the worst case determination procedure detailed below. In summary, the xy plane is the exposure plane, and z axis is the vector in propagation direction towards the body.

3.4.1 Terminology:

- Element – each one of the radiating elements that are used in the system (the antenna array has 16 radiating elements). We denote the antenna element with index **k** in this explanation.
- **N** – number of chains in the RFEM 2, **N**=16.
- Point – each point on the grid that is used for searching for the worst case position. The points are spaced 0.1mm from each other. The grid point would be denoted as **g** in this explanation.
- Complex E field vector generated by the kth antenna element at point g :
- Complex H field vector generated by the kth antenna element at point g :

$$\vec{E}_{k,g} = \hat{x}(\text{Re}[E_{kx,g}] + j\text{Im}[E_{kx,g}]) + \hat{y}(\text{Re}[E_{ky,g}] + j\text{Im}[E_{ky,g}]) + \hat{z}(\text{Re}[E_{kz,g}] + j\text{Im}[E_{kz,g}])$$

$$\vec{H}_{k,g} = \hat{x}(\text{Re}[H_{kx,g}] + j\text{Im}[H_{kx,g}]) + \hat{y}(\text{Re}[H_{ky,g}] + j\text{Im}[H_{ky,g}]) + \hat{z}(\text{Re}[H_{kz,g}] + j\text{Im}[H_{kz,g}])$$

- \hat{x} , \hat{y} , \hat{z} – are unit direction vectors having unit magnitude and are mutually orthogonal to each other.
- Without loss of generality in this explanation RFEM 2 and search plane are in the \hat{x} , \hat{y} plane and the integrated 1cm² plane is perpendicular to \hat{z} direction.

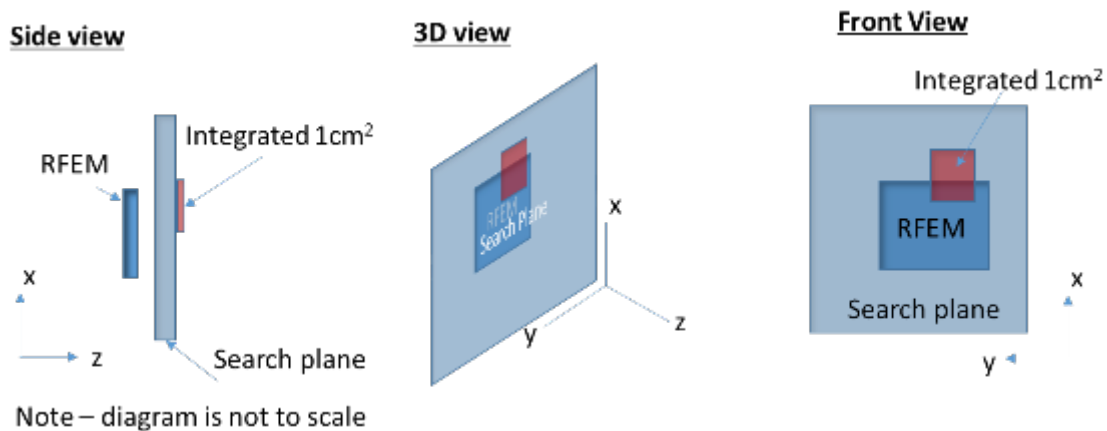


Figure 4 – Near field worst case terminology and orientation



3.4.2 Primer on field vector representation:

E and H fields generated by the k chain are:

$$\vec{E}_k = \vec{x}(\text{Re}[E_{kx}] + j\text{Im}[E_{kx}]) + \vec{y}(\text{Re}[E_{ky}] + j\text{Im}[E_{ky}]) + \vec{z}(\text{Re}[E_{kz}] + j\text{Im}[E_{kz}])$$

$$\vec{H}_k = \vec{x}(\text{Re}[H_{kx}] + j\text{Im}[H_{kx}]) + \vec{y}(\text{Re}[H_{ky}] + j\text{Im}[H_{ky}]) + \vec{z}(\text{Re}[H_{kz}] + j\text{Im}[H_{kz}])$$

E and H fields generated by all N chains are

$$\vec{E}_{\text{All}} = \vec{x} \sum_{k=1}^N (\text{Re}[E_{kx}] + j\text{Im}[E_{kx}]) + \vec{y} \sum_{k=1}^N (\text{Re}[E_{ky}] + j\text{Im}[E_{ky}]) + \vec{z} \sum_{k=1}^N (\text{Re}[E_{kz}] + j\text{Im}[E_{kz}])$$

$$\vec{H}_{\text{All}} = \vec{x} \sum_{k=1}^N (\text{Re}[H_{kx}] + j\text{Im}[H_{kx}]) + \vec{y} \sum_{k=1}^N (\text{Re}[H_{ky}] + j\text{Im}[H_{ky}]) + \vec{z} \sum_{k=1}^N (\text{Re}[H_{kz}] + j\text{Im}[H_{kz}])$$



Poynting vector generated by all N chains is

$$\begin{aligned}
\overrightarrow{P_{\text{General,All}}} &= \frac{1}{2} \overrightarrow{E_{\text{All}}} \times \overrightarrow{H_{\text{All}}}^* \\
&= \frac{1}{2} \langle \vec{x} \left\{ \sum_{k=1}^N (\text{Re}[E_{ky}] + j\text{Im}[E_{ky}]) \sum_{k=1}^N (\text{Re}[H_{kz}] - j\text{Im}[H_{kz}]) \right. \\
&\quad - \sum_{k=1}^N (\text{Re}[E_{kz}] + j\text{Im}[E_{kz}]) \sum_{k=1}^N (\text{Re}[H_{ky}] - j\text{Im}[H_{ky}]) \left. \right\} \\
&\quad + \vec{y} \left\{ \sum_{k=1}^N (\text{Re}[E_{kz}] + j\text{Im}[E_{kz}]) \sum_{k=1}^N (\text{Re}[H_{kx}] - j\text{Im}[H_{kx}]) \right. \\
&\quad - \sum_{k=1}^N (\text{Re}[E_{kx}] + j\text{Im}[E_{kx}]) \sum_{k=1}^N (\text{Re}[H_{kz}] - j\text{Im}[H_{kz}]) \left. \right\} \\
&\quad + \vec{z} \left\{ \sum_{k=1}^N (\text{Re}[E_{kx}] + j\text{Im}[E_{kx}]) \sum_{k=1}^N (\text{Re}[H_{ky}] - j\text{Im}[H_{ky}]) \right. \\
&\quad \left. - \sum_{k=1}^N (\text{Re}[E_{ky}] + j\text{Im}[E_{ky}]) \sum_{k=1}^N (\text{Re}[H_{kx}] - j\text{Im}[H_{kx}]) \right\} \rangle
\end{aligned}$$

Power flow is

$$\begin{aligned}
\text{Re}[\overrightarrow{P_{\text{General,All}}}] &= \frac{1}{2} \langle \vec{x} \left\{ \sum_{k=1}^N \text{Re}[E_{ky}] \sum_{k=1}^N \text{Re}[H_{kz}] + \sum_{k=1}^N \text{Im}[E_{ky}] \sum_{k=1}^N \text{Im}[H_{kz}] - \sum_{k=1}^N \text{Re}[E_{kz}] \sum_{k=1}^N \text{Re}[H_{ky}] \right. \\
&\quad \left. - \sum_{k=1}^N \text{Im}[E_{kz}] \sum_{k=1}^N \text{Im}[H_{ky}] \right\} \\
&\quad + \vec{y} \left\{ \sum_{k=1}^N \text{Re}[E_{kz}] \sum_{k=1}^N \text{Re}[H_{kx}] + \sum_{k=1}^N \text{Im}[E_{kz}] \sum_{k=1}^N \text{Im}[H_{kx}] - \sum_{k=1}^N \text{Re}[E_{kx}] \sum_{k=1}^N \text{Re}[H_{kz}] \right. \\
&\quad \left. - \sum_{k=1}^N \text{Im}[E_{kx}] \sum_{k=1}^N \text{Im}[H_{kz}] \right\} \\
&\quad + \vec{z} \left\{ \sum_{k=1}^N \text{Re}[E_{kx}] \sum_{k=1}^N \text{Re}[H_{ky}] + \sum_{k=1}^N \text{Im}[E_{kx}] \sum_{k=1}^N \text{Im}[H_{ky}] - \sum_{k=1}^N \text{Re}[E_{ky}] \sum_{k=1}^N \text{Re}[H_{kx}] \right. \\
&\quad \left. - \sum_{k=1}^N \text{Im}[E_{ky}] \sum_{k=1}^N \text{Im}[H_{kx}] \right\} \rangle
\end{aligned}$$

Power flow to Z is

$$\begin{aligned}
\vec{z} \cdot \text{Re}[\overrightarrow{P_{\text{General,All}}}] &= \frac{1}{2} \langle \left\{ \sum_{k=1}^N \text{Re}[E_{kx}] \sum_{k=1}^N \text{Re}[H_{ky}] + \sum_{k=1}^N \text{Im}[E_{kx}] \sum_{k=1}^N \text{Im}[H_{ky}] - \sum_{k=1}^N \text{Re}[E_{ky}] \sum_{k=1}^N \text{Re}[H_{kx}] \right. \\
&\quad \left. - \sum_{k=1}^N \text{Im}[E_{ky}] \sum_{k=1}^N \text{Im}[H_{kx}] \right\} \rangle
\end{aligned}$$



3.4.3 Domain search for worst case direction

The two domain search is completed as follows:

- A. First find a direction (location) for the worst case 1cm² square averaging area using upper bound methods.
The basic concept behind the upper bound method is to assume that there could be an “ideal beam forming” mechanism that could align the phases of all the elements for both E and H field (obviously in real life this cannot happen – this is the reason that this is an upper bound method). When this ideal mechanism is used then all the complex phasors are aligned to the same phase, hence the phasor absolute value can be used instead of the phasor -> the E (and H) field for any direction is the sum of the magnitude of the fields (look at item 3 below for more formal description).
This method provides the worst case position independent of the antenna phases -> it allows finding the worst case location with this “ideal beam forming” mechanism.
Item 3 below translate the above verbal description to more formal mathematical wording.
- B. After the worst case direction is found using the upper bound method, the antenna phases are aligned to this direction. The antenna phases are aligned to maximize the power across the 1cm² averaging area that was found using the upper bound method. The method that is used to find the required antenna phases is: first order the antenna according to the power contribution on the found 1cm² from the highest to the lowest. Then start by activating the antenna that contribute the most and set its phase to 0, then activate the 2nd antenna and search over the phases for the 2nd antenna. Choose the phase that maximize the power of the two antenna elements. For finding the phase for the third antenna fix antenna 1 phase to zero and the 2nd antenna to the value that was found before – now search for the phases for the third antenna phases that maximize the power. Continue with the same process till the 16th element.
- C. Calculate the power density with the antenna phases that were found in the previous item (item B).

The above process can be written as the following algorithm:

1. A grid is defined with 0.1mm spacing.
2. At each point in the grid, the complex E & H fields are calculated using each one of the 16 radiating elements separately. Each one of the calculated E & H fields are 3D complex vectors, so the simulation output from this stage is 16 3-D complex E field strength vectors and 16 3D complex H field strength vectors. The vectors are defined as:

$$\vec{E}_{k,g} = \vec{x}(\text{Re}[E_{kx,g}] + j\text{Im}[E_{kx,g}]) + \vec{y}(\text{Re}[E_{ky,g}] + j\text{Im}[E_{ky,g}]) + \vec{z}(\text{Re}[E_{kz,g}] + j\text{Im}[E_{kz,g}])$$

$$\vec{H}_{k,g} = \vec{x}(\text{Re}[H_{kx,g}] + j\text{Im}[H_{kx,g}]) + \vec{y}(\text{Re}[H_{ky,g}] + j\text{Im}[H_{ky,g}]) + \vec{z}(\text{Re}[H_{kz,g}] + j\text{Im}[H_{kz,g}])$$
3. Upper bound assumption is used to derive the E & H field on each one of the grid point, the following items describe the upper bound method that is used:
 - a. The calculation is made separately for E field and H field.
 - b. For E field the following calculation is made independently for each one of the grid point:

$$\vec{E}_{UB,g} = \vec{x} \sum_{k=1}^N \sqrt{\text{Re}[E_{kx,g}]^2 + \text{Im}[E_{kx,g}]^2} + \vec{y} \sum_{k=1}^N \sqrt{\text{Re}[E_{ky,g}]^2 + \text{Im}[E_{ky,g}]^2} + \vec{z} \sum_{k=1}^N \sqrt{\text{Re}[E_{kz,g}]^2 + \text{Im}[E_{kz,g}]^2} = \vec{x} \sum_{k=1}^N |E_{kx}| + \vec{y} \sum_{k=1}^N |E_{ky,g}| + \vec{z} \sum_{k=1}^N |E_{kz,g}|$$

The magnitude of the complex E vector is summed over the antenna elements. The summation is being done for each one of the grid point and for each one for each direction independently.

- c. The output of the previous item is 3D real vector of the E field on each one of the simulated grid points in each direction. The physical implementation is that an ideal beam forming was done for the E field for each one of the points.
- d. Same process as described in item b is being done for the H field.

$$\begin{aligned} \vec{H}_{UB,g} = \hat{x} \sum_{k=1}^N \sqrt{\text{Re}[H_{kx,g}]^2 + \text{Im}[H_{kx,g}]^2} + \hat{y} \sum_{k=1}^N \sqrt{\text{Re}[H_{ky,g}]^2 + \text{Im}[H_{ky,g}]^2} \\ + \hat{z} \sum_{k=1}^N \sqrt{\text{Re}[H_{kz,g}]^2 + \text{Im}[H_{kz,g}]^2} = \hat{x} \sum_{k=1}^N |H_{kx,g}| + \hat{y} \sum_{k=1}^N |H_{ky,g}| + \hat{z} \sum_{k=1}^N |H_{kz,g}| \end{aligned}$$

- e. In each point in the grid the poynting vector is calculated by vector multiplication of E & H field which are added-up in items b & d. As explained before, without loss of generality we assume that the search plane is X/Y plane and the energy propagate to Z dimension, this translates to:

$$\begin{aligned} P_{g,z} &= \frac{1}{2} \text{Re}\{\hat{z} \cdot (\vec{E} \times \vec{H}^*)\} = \frac{1}{2} \text{Re}\{\hat{z} \cdot ((\dots)\hat{x} + (\dots)\hat{y} + (E_x H_y^* - E_y H_x^*)\hat{z})\} = \\ &= \frac{1}{2} \text{Re}\{E_x H_y^* - E_y H_x^*\} \leq \frac{1}{2} |E_x H_y^* - E_y H_x^*| \leq \\ &\leq \frac{1}{2} |E_x H_y^*| + \frac{1}{2} |E_y H_x^*| = \frac{1}{2} \{|E_x| \cdot |H_y| + |E_y| \cdot |H_x|\} = \\ P_{UpperBound_{z,g}} &= \frac{1}{2} \langle \sum_{i=1}^N |E_{ix}| \sum_{i=1}^N |H_{iy}| + \sum_{i=1}^N |E_{iy}| \sum_{i=1}^N |H_{ix}| \rangle \end{aligned}$$

The final value $(\frac{1}{2} \langle \sum_{i=1}^N |E_{ix}| \sum_{i=1}^N |H_{iy}| + \sum_{i=1}^N |E_{iy}| \sum_{i=1}^N |H_{ix}| \rangle)$ obtained in each grid point represents an upper bound value i.e. this value is always greater than or equal to the real pointing vector magnitude $(\frac{1}{2} \text{Re}\{\hat{z} \cdot (\vec{E} \times \vec{H}^*)\})$.

4. The above calculated Poynting vectors are used to estimate the power across 1cm² area. Note that in this example the relevant direction for the pointing vector is \hat{z} direction

$$P_{1cm^2} = \iint_{1cm^2} \overline{P_{UpperBound_{g_{x,y,z}}}} \cdot \hat{z}$$

5. The 1cm² area with the highest power value is used as the worst case the direction. The antenna phases are aligned to maximize the energy in this 1cm² area as explained below:

- a. Turn on each element one-by-one to find order of power intensity in the 1cm² window. (Find the order of contribution)
- b. Sort in the power order from the highest to the lowest #0 to #15.
- c. Turn on #0 with phase P0=0. (reference)
- d. Turn on #1 and change phase to maximize the power and find the phase P1.
- e. Keep P0 and P1, turn on #2 and do same.
- f. Repeat for the rest of the antennas.

6. Using the antenna phases that were calculated in step 6 the power density is calculated along the base plane.

3.5 Worst case operating conditions of the platform

The platform Lenovo TP00078A is a special platform with the ability to rotate the screen by 360°. This ability allows the platform to work in various operation modes, as illustrated in the Figure 5.



Figure 5 – Platform operating modes

The worst case condition regarding the radiated near field was found for Tablet operating mode. When Tablet operating mode is set, the lid is rotated by 360 where the screen is folded over on top of the keyboard as shown on the Figure 6.



Figure 6 - Platform worst case operating mode

3.6 3D models used in the simulation

3.6.1 RFEM 2 housing inside Intel 18260NGW module

3D Intel 18260NGW module CAD files are used in the EM simulation to allow correct exposure level simulation.

Please refer to the following picture only as a reference to visualize RFEM 2 placement inside the Lenovo Model TP00078A platform.



Figure 7– Active antenna inside the platform

3.6.2 Antenna distance to the body of an end user

The highest RF exposure was found when the platform is configured in tablet mode, the screen is flipped to the backside of the keyboard. The minimum distance between the active antennas to the skin of an end user is when the person holding the unit and touching the plastic. For this configuration, 2 planes have been simulated, one on the base as shown on the Figure 8 and the second one on as shown on the Figure 9. The minimum distance between a hand or body to the active antenna is 14.27 mm for the simulated plane on the base and 8.46 mm for the simulated plane on edge.



Figure 8 - Simulated area on the base



Figure 9 - Simulated area on the edge

3.6.3 Metals in proximity of the RFEM 2

All the metals that are in the RFEM 2 region (10mm on each side) were included in the simulation.



3.7 Antenna feed

The following gives a general description of the numerical simulations; other details of the simulation geometry are included in the confidential Operational Description exhibit. The EM simulation uses an accurate 3D model of the RFEM 2 antenna. The model includes the antenna elements as well as their feeding lines. Both PCBs (antenna PCB and Si PCB) are simulated. The simulation starts at the silicon bumps (the metal bump that is connected to the Silicon and soldered to the board).

In the simulation, we excite the antennas at the silicon output port (the antenna structure includes the vias, traces and actual antenna element). Please note that the output ports are used as the interface from the Si to the antenna. The Si output are localized in the Si side, while looking from the PCB + antenna direction we can find the antenna feed points. The RFEM layers are fully simulated, including all parts of the PCB and antennas boards: conducted traces, feeds, antenna elements and dielectrics. The mesh resolution is automatically defined by the simulation tool to assure better than 2% simulation convergence precision.

Signals with equal level are applied for the 16 antenna chains. The simulation uses a fixed power feed per element, such that the aggregated conducted output power at the antenna feed points is 6.6 dBm. In other words each one of the 16 elements is fed by -5.4 dBm such that the total conductive equivalent power is 16 times -5.4 dBm, so +6.6 dBm. In addition, the simulation is conducted using 100% TX duty cycle.

The total power (same per element) is used to build the pattern of radiated power through beam forming. For building the beamforming pattern the same power is used per element, while phase is changed per element, please look at chapter 2.2 for more information about the beamforming. Phases are derived for each excitation separately to simulate the worst case condition. Chapter 3.4 explains how the phases are derived to find worst case condition.

4 Simulation Results

As described in the section 3.6.2 two planes have been simulated, the power density of both planes results are presented in this section. (z axis is the direction orthogonal to the body).

The power density has been simulated over 3 channels, for each channel we'll present the results detail according to the methodology explained in section 3.4:

- Simulation results of the single-point power density for each spot across the Mesh ($PUpperBound_{z,g}$) and the worst case coordinate (Figure 11 to Figure 13 for edge plane and Figure 25 to Figure 27 for base plane). Please note that this value is single-point power density and not integrated power density over 1cm^2 (even though mW/cm^2 scale is used, this value represents an upper bound power density for each spot of the mesh which is much smaller area than 1cm^2).
- The results of the single-point power density in z direction using the antenna phases corresponding to the worst case coordinate found above (Figure 15 to Figure 17 for edge plane and Figure 28 to Figure 30 for base plane). In this section correction factors are presented, these factors are the ratios between the single-point power density using the z component of Poynting vector and the single-point power density using the three components of Poynting vector. These factors are presented in Table 3 of section 4.1.2 and Table 7 of section 4.2.2.
- One dimensional cut of the mesh single-point power density – showing 1 dimensional cut of the mesh power density (Figure 18 to Figure 20 for edge plane and Figure 31 to Figure 33 for base plane). In the XY plane, the X cut is done with the Y in the maximum value, similarly Y cut is done with the X in the maximum value. These results show the results using the z component of the Poynting vector.
- Integrated power density over 1cm^2 – these figures present the integrated power density across 1cm^2 using the z component of Poynting vector (Figure 21 to Figure 23 for edge plane and Figure 34 to Figure 36 for base plane). Each point in the figure represents integration over 1cm^2 , where the point location is the location of the center of the square
- The worst case power-density in z direction integrated over 1cm^2 using the worst case antenna phases computed by the simulation (Table 4 for edge plane and Figure 37 to Figure 39 for base plane) and the final value at zero distance obtained by the application of the scaling factors between normal and global Poynting vector components. (Table 5 for edge plane and Table 8 for base plane).

4.1 Results on the edge area.

In this section are presented the simulation results of the platform configured in tablet mode. The area simulated is located on the edge, as shown in blue on the Figure 10. Z direction (Beam direction) is the direction towards the body.



Figure 10 – Edge plane illustration

4.1.1 Upper bound simulation results

The Figure 11, Figure 12 and Figure 13 present upper bound Z single-point power density as described in section 3.4

Please note that since the worse-case conditions are searched over a plane for near field, then the azimuth and the elevation are not relevant. The worst case position is calculated using all the power density single-point issued from the upper bound simulation results. The upper bound worst case Z power density distributions for three channels are shown in Figure 11, Figure 12 and Figure 13. We leverage the phase conditions (summarized in Table 2) for each antenna element that resulted in these worst case conditions to evaluate final integrated power density. The mathematical basis for using these as the worst case phase conditions to evaluate the final integrated power density is provided in Section 3.4.3.

The plane dimensions of the Z single-point power density results is 49.5 mm x 32.4 mm (Figure 11, Figure 12 and Figure 13).

The footprint of the components in the edge plane for single-point power density representation is showed in Figure 14.

Worst case coordinates on channel 1 are $x=27.2$ mm, $y= 27$ mm.

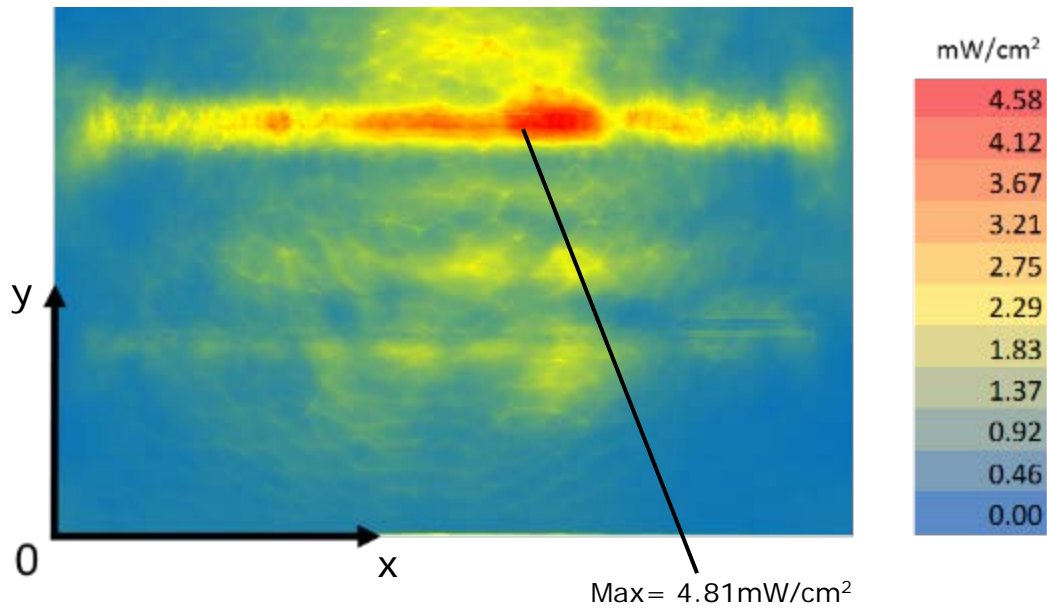


Figure 11 – Channel 1 upper bound, Single-point power density mesh on platform edge at 100% duty cycle

Worst case coordinates on channel 2 are $x=27$ mm , $y=27$ mm.

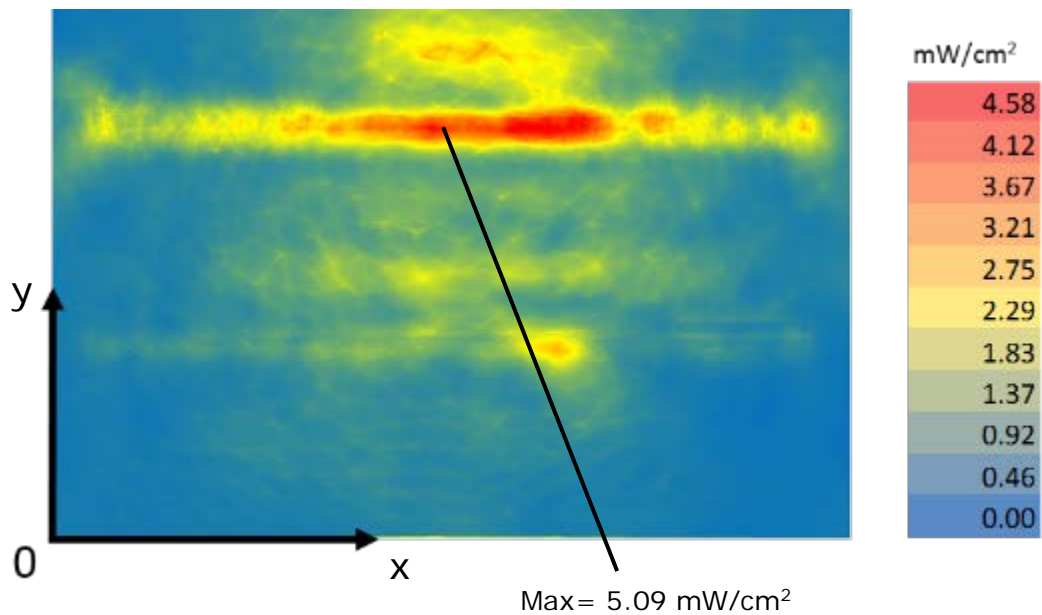


Figure 12 – Channel 2 upper bound, Single-point power density mesh on platform edge at 100% duty cycle



Worst case coordinates on channel 3 are $x=27.4$ mm, $y=27$ mm.

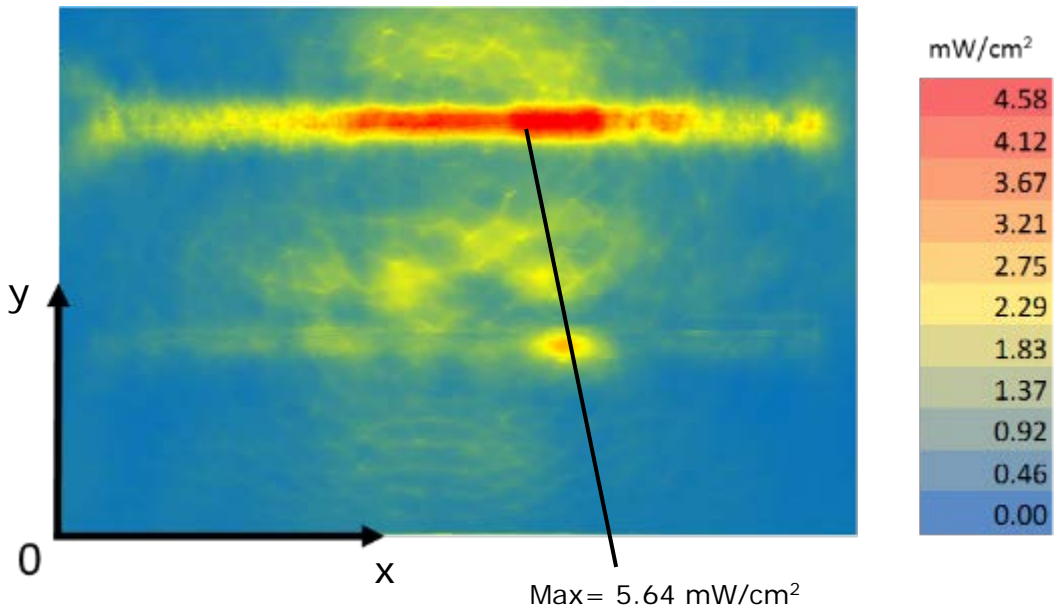


Figure 13 – Channel 3 upper bound, Single-point power density mesh on platform edge at 100% duty cycle



Figure 14 – Footprint in edge plane



4.1.2 Single-point power density values with worst-case antenna phases for edge plane exposure

The Table 2 shows the phase for each antenna elements per channel for the worst case found as described in the chapter 3.4. The phases search algorithm is detailed in point 5 of the section 3.4.3

Antenna index	Phases [Degrees]		
	Channel 1	Channel 2	Channel 3
0	315	135	225
1	45	180	315
2	180	225	90
3	0	0	270
4	90	45	135
5	180	90	180
6	270	180	180
7	45	0	270
8	180	315	180
9	270	45	270
10	45	135	0
11	225	270	180
12	45	270	315
13	45	0	45
14	135	135	90
15	270	270	225

Table 2 - Phases configurations for the worst case

The amplitude on each antenna is -5.4dBm as explained in chapter 3.7.

The Figure 15, Figure 16 and Figure 17 present power density in the body direction using worst case antenna phases presented in the Table 2. The simulated power density area has a size of is 49.5 mm x 32.4 mm, this area corresponds to the blue delimitation.



Table 3 presents the ratios (linear and logarithmic) at the highest spot value for the Z trajectory on the edge area between the power density worst case value along the body direction (S_z) and the power density worst case value along the propagation direction (S_{tot}) for all channels and taking into account all components. This table confirms that the power density component along Z is the principal contributor in the total power density. Also the ratios are used for results scaling in Table 5 of section 4.1.5 and in the compliance summary discussion in Clause 6.

EDGE AREA	Channel 1	Channel 2	Channel 3
Mag S_{tot} (maximum poynting spot value with all components) [mW/cm ²]	1.509	1.387	1.521
S_z (trajectory of the above on Z direction) [mW/cm ²]	1.279	1.261	1.307
Ratio (S_z / S_{tot}) (linear)	0.847	0.909	0.860
Ratio $10\log(S_z / S_{tot})$ (dB)	-0.72	-0.41	-0.66

Table 3 – Ratios between Z-power density and total power density on edge area



Worst case coordinates on channel 1 are $x=28.1$ mm, $y=17.8$ mm.

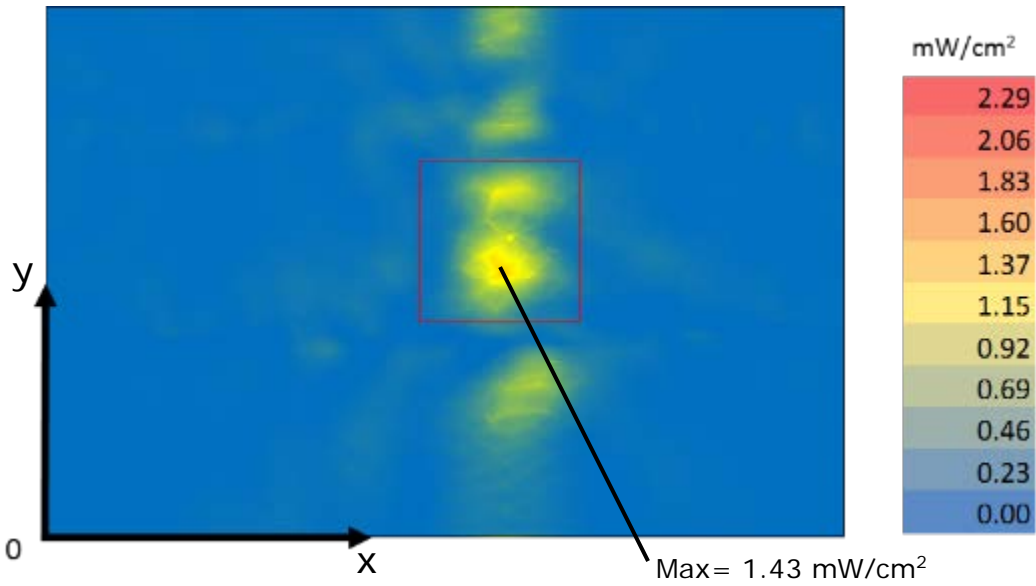


Figure 15 – Channel 1 single-point power density mesh on platform edge

Worst case coordinates on channel 2 are $x=23.5$ mm, $y=17.1$ mm.

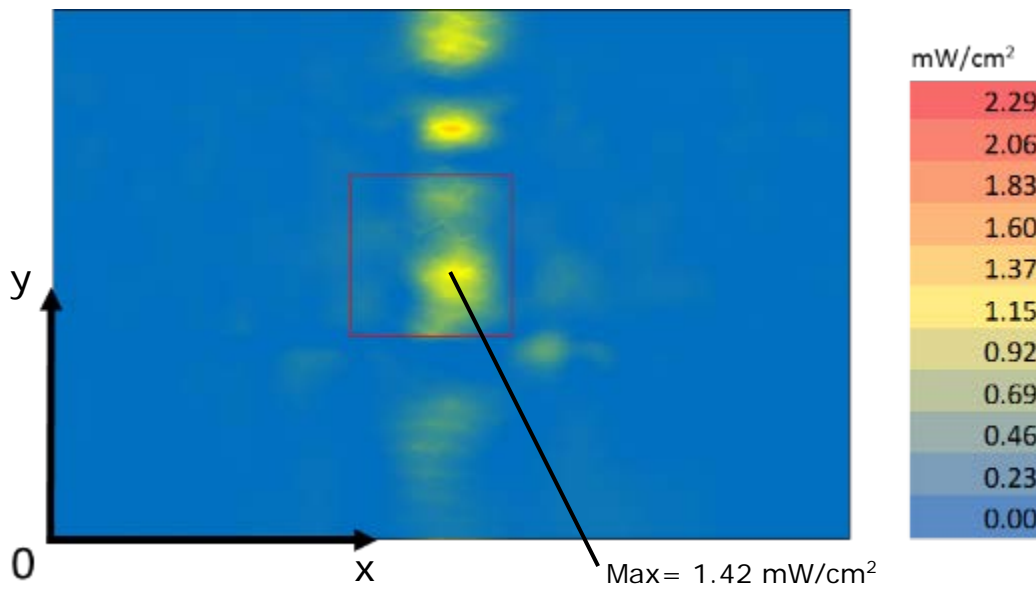


Figure 16 – Channel 2 single-point power density mesh on platform edge

Worst case coordinates on channel 3 are $x=28.1$ mm, $y=18.3$ mm.

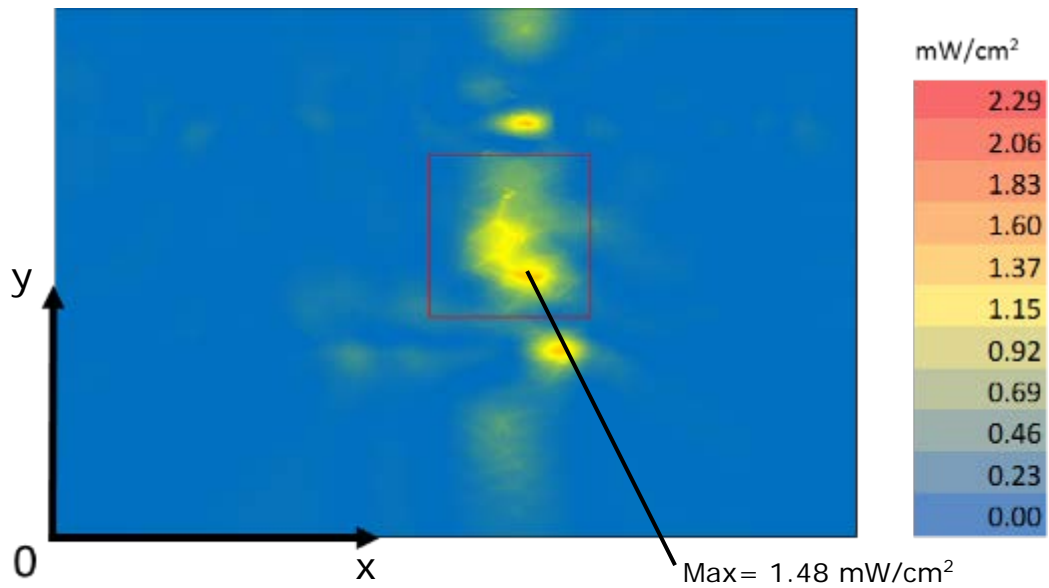


Figure 17 – Channel 3 single-point power density mesh on platform edge

The highest value shown in these figures is a point and not yet integrated over the 1cm^2 . The final power density value is given in section 4.1.5.

4.1.3 One dimensional cut of the mesh single-point power density for edge plane exposure

In Figure 18 – Figure 20 below, we present a subset of the simulation results from the Z component of single-point power density values with worst antenna phases (Chapter 4.1.2).

The subset is a 1 dimensional cut in the X axis and Y axis that shows the behavior of the near field power density at zero distance.

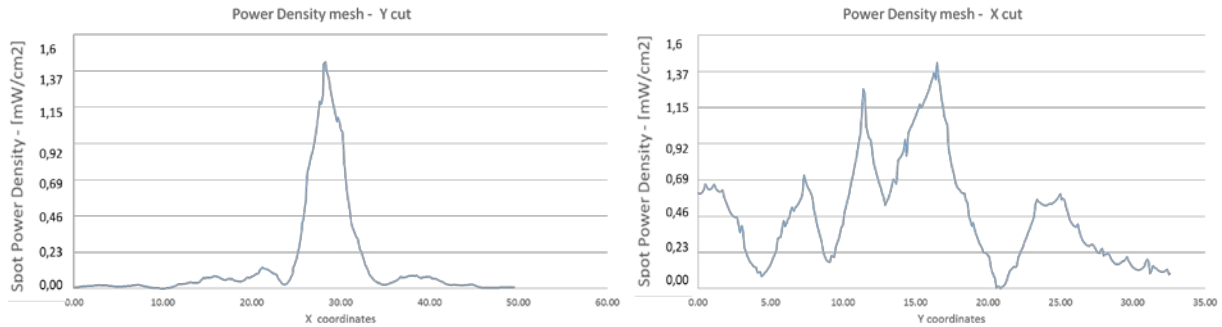


Figure 18 - One dimensional plots of the power density on Channel 1

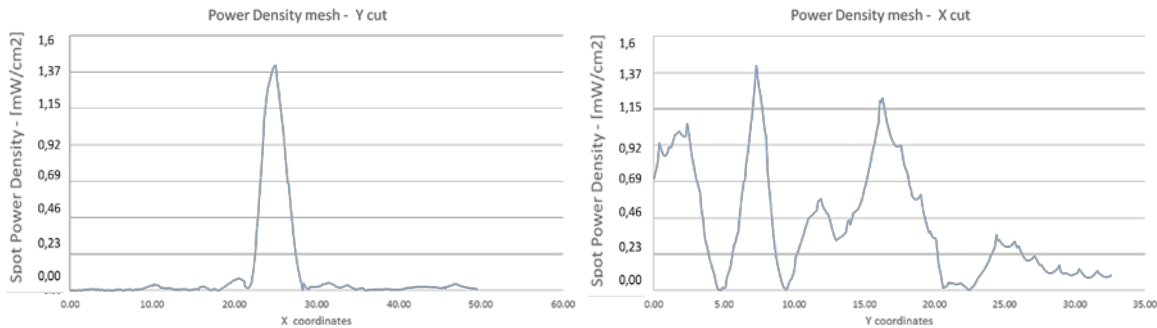


Figure 19 - One dimensional plots of the power density on Channel 2

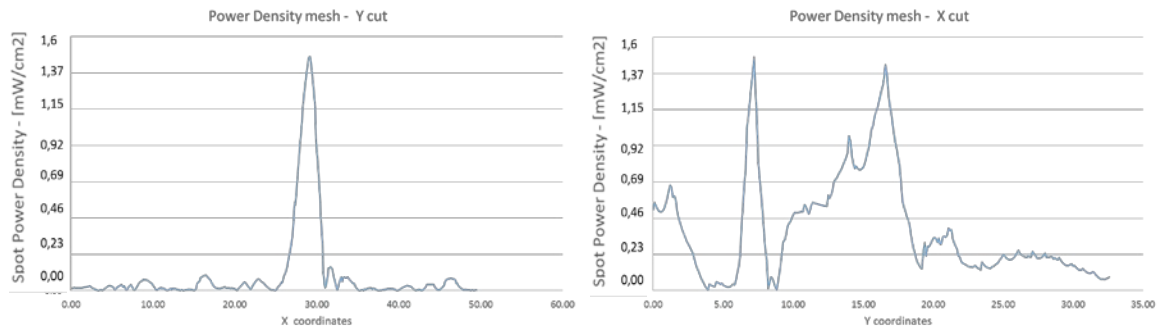


Figure 20 - One dimensional plots of the power density on Channel 3

4.1.4 Integrated power density over 1 cm² for edge plane exposure

The Figure 21 - Figure 23 below present the Z-integrated power over 1cm² at 100% duty cycle for the worst case scenario as explained in section 3.4.3. The plane dimensions of these results is 39.5 mm x 22.4 mm. These figures show also by transparency the structure drawing of the laptop, such as materials and RFEM 2 antenna used in simulation.

The 1cm² square location correspondent to the maximum of integrated power density value for each channel is plotted in red in figures below (Figure 21 - Figure 23). The maximum average values are mentioned in the second row of Table 4. The worst case coordinates are the center of the squares.

Worst case coordinates on channel 1 are x=23.1 mm,y=12.9 mm.

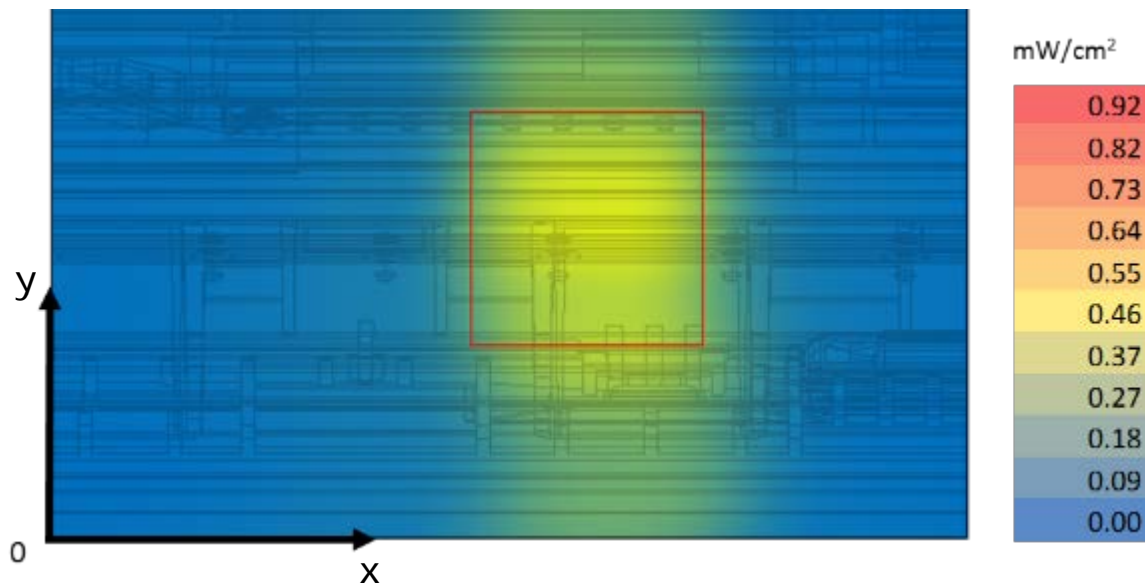


Figure 21 – Channel 1 worst case - Integrated power over 1cm² an platform edge

Worst case coordinates on channel 2 are x=18.5 mm, y=12.2 mm.

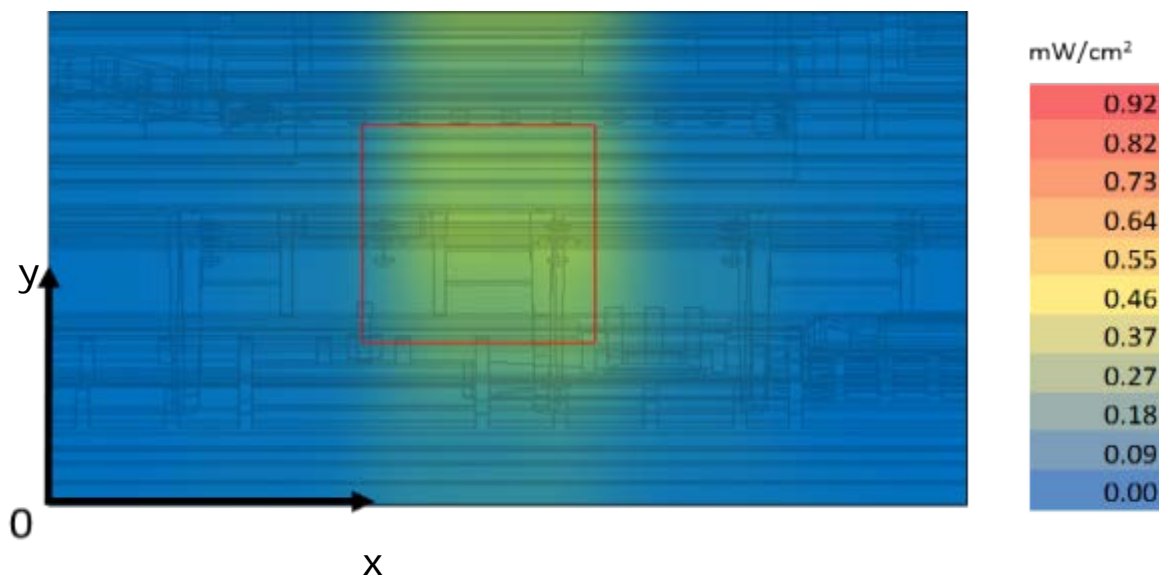


Figure 22 – Channel 2 worst case - Integrated power over 1cm² an platform edge



Worst case coordinates on channel 3 are $x=23.1$ mm, $y=13.4$ mm.

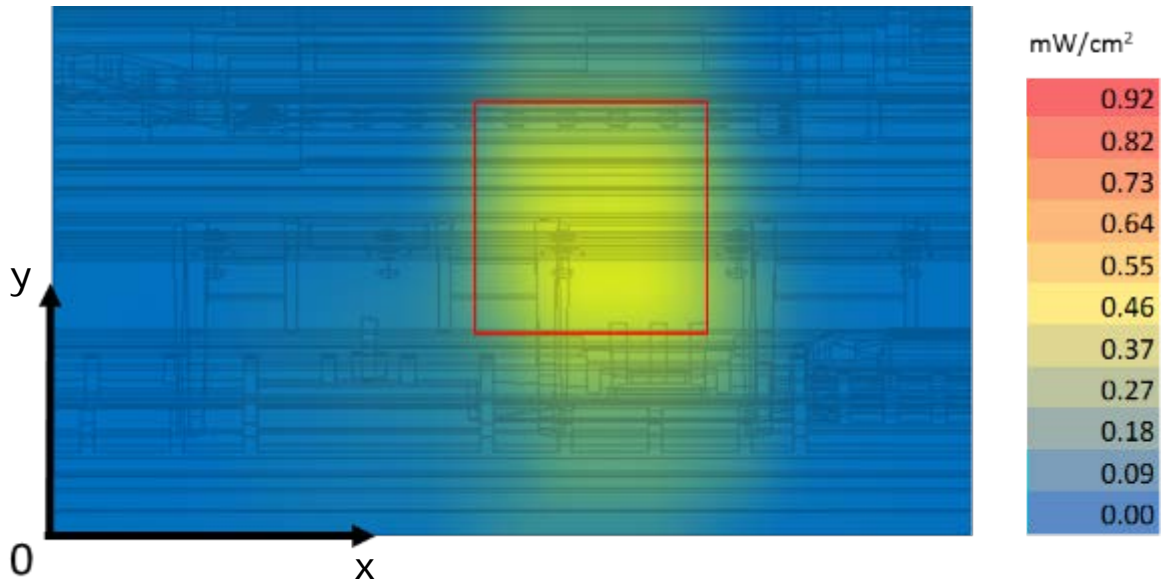


Figure 23 – Channel 3 worst case - Integrated power over 1cm² on a platform edge

4.1.5 Power density

The Table 4 shows the worst case power-density in the edge plane. As described in section 3.4 and section 3.6.2 the worst case was computed by the simulation using the worst case antenna phases and the worst platform configuration (Tablet mode). The 0mm reference correspond to the platform boundary, the active antenna located inside the platform is at 8.46 mm from this distance.

Note that for the edge plane only the power density averaged values in the plane are presented in a form of table (Table 4). However for the base plane the power densities values are presented versus the distances in a form of graphs because the base plane is the worst case exposure plane for which we had performed the correlation simulation vs measurement for several distances from the transition-zone field to far field.

Table 4 - Worst case power density - Edge plane

Edge plane Highest power density	Channel 1 [mW/cm ²]	Channel 2 [mW/cm ²]	Channel 3 [mW/cm ²]
70% duty cycle	0.32	0.38	0.29
100% duty cycle	0.46	0.54	0.41

Notes for Table 4:

1. The worst case channel is channel 2.
2. The Maximum power density (spatially integrated over worst 1cm²) in channel 2 (worst case) is achieved at 0mm distance from the platform boundary and equals to 0.54mW/cm² over 100% duty cycle.
3. As explained in section 2.3, the Intel 18260NGW module is limited to Transmit at a duty cycle of 70% over 10 seconds. Therefore the maximum spatially integrated and time averaged power density over 1cm² is $0.54 * 0.7 = 0.38\text{mW/cm}^2$.
4. Taking into account the ratios presented in Table 3 between the Z-component and the total power density, the integrated power densities values at zero distances become:

	Channel 1	Channel 2	Channel 3
Integrated Power density in Z-direction (P_z) [mW/cm ²]	0.32	0.38	0.29
Corresponding Ratio (R)	0.847	0.909	0.860
Global Integrated Power density ($P_{tot}=P_z/R$) [mW/cm ²]	0.378	0.418	0.337

Table 5 –Edge plane integrated power density at zero distance

Therefore, the worst case channel remains channel 2 and the maximum spatially integrated and time averaged total power density over 1cm² is $0.38 / 0.909=0.418 \text{ mW/cm}^2$.

4.2 Results on the base area.

In this section are presented the simulation results of the platform configured in tablet mode. The area simulated is located on the base, as shown in blue on the Figure 24. Z direction (Beam direction) is the direction towards the body.

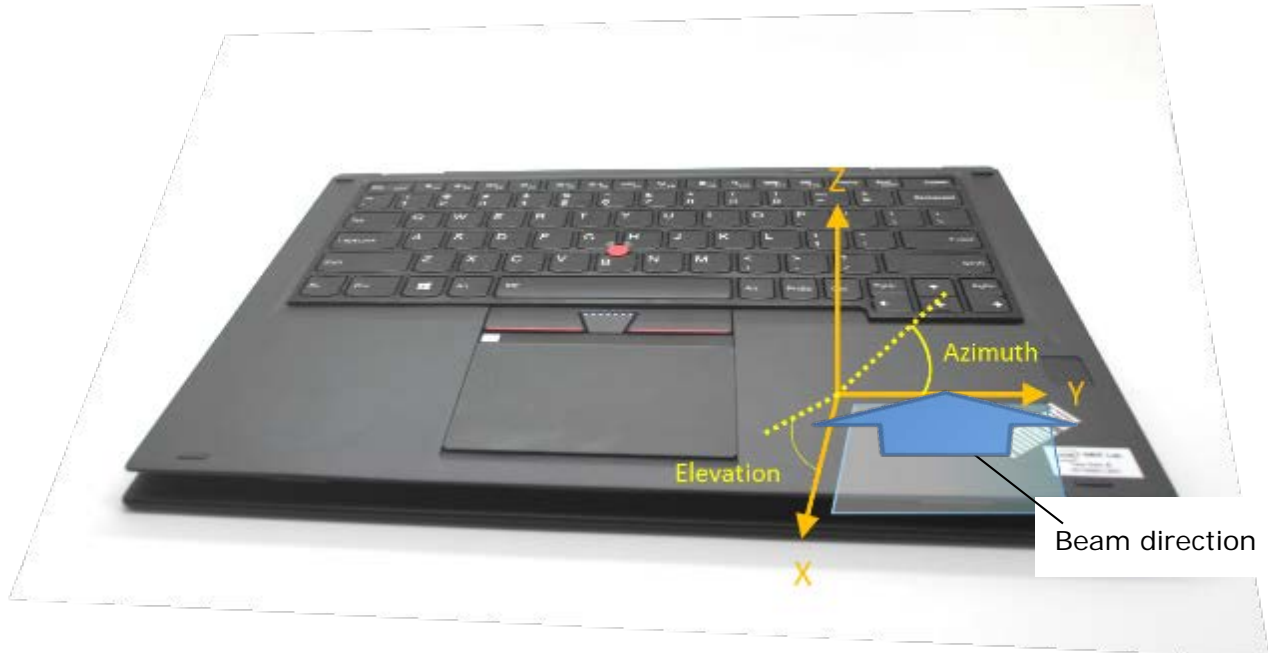


Figure 24 – Elevation and azimuth angles

4.2.1 Upper bound simulation results

The figures below present upper bound Z single-point power density (as described in section 3.4). In each figure the single point power (in mW/cm^2) is shown as well as the place of this maximum value.

Please note that since the worst-case conditions are searched over a plane for near field, then the azimuth and the elevation are not relevant. The worst case position is calculated using all the power density spot issued from the upper bound simulation results. The upper bound worst case Z power density distributions for three channels are shown in Figure 25, Figure 26 and Figure 27. We leverage the phase conditions (summarized in Table 6) for each antenna element that resulted in these worst case conditions to evaluate final integrated power density. The mathematical basis for using these as the worst case phase conditions to evaluate the final integrated power density is provided in Section 3.4.3.

The plane dimensions of the single-point power density results is 49.5 mm x 32.4 mm (Figure 25, Figure 26 and Figure 27).

Worst case coordinate on channel 1 is at $x=27.9$ mm, $y=18.3$ mm.

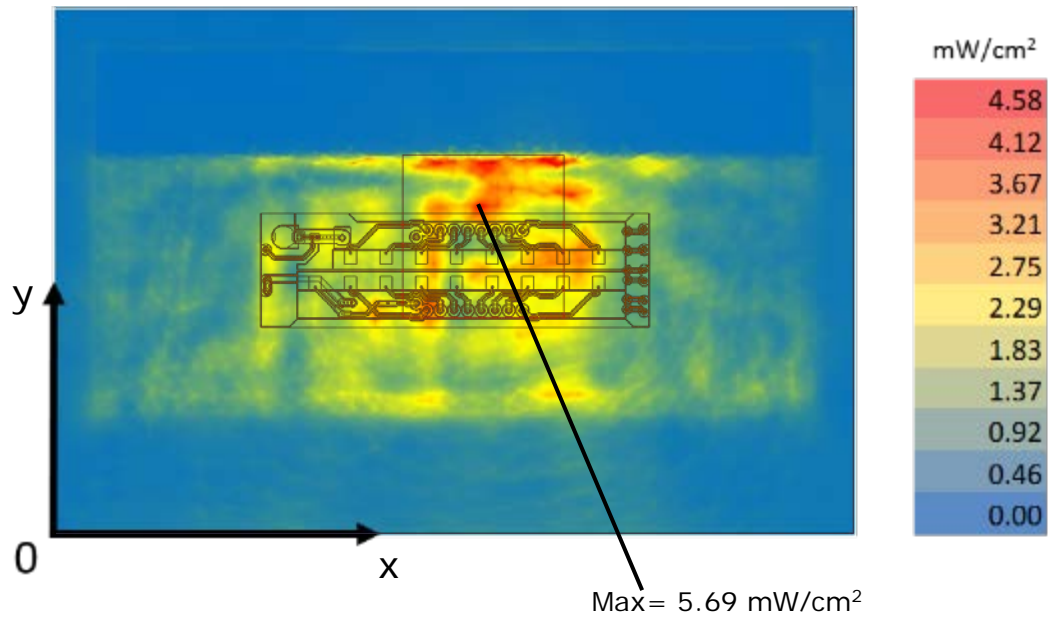


Figure 25 – Channel 1 upper bound, Single-point power density mesh on platform base at 100% duty cycle

Worst case coordinates on channel 2 are $x=28$ mm, $y= 18.2$ mm.

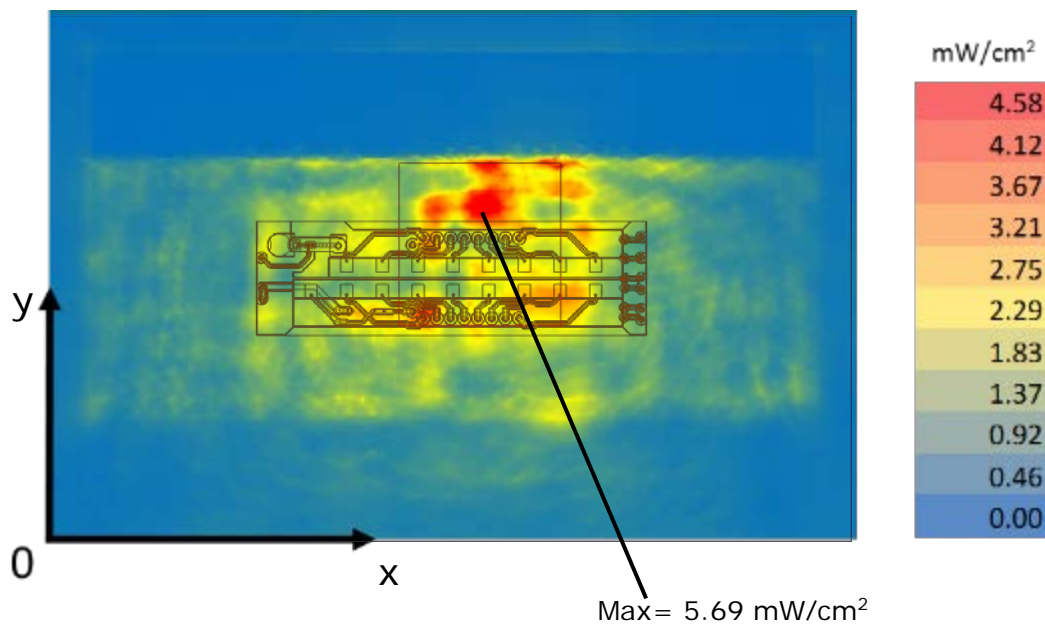


Figure 26 – Channel 2 upper bound, Single-point power density mesh on platform base at 100% duty cycle



Worst case coordinates on channel 3 are $x=22.5$ mm, $y=13.2$ mm.

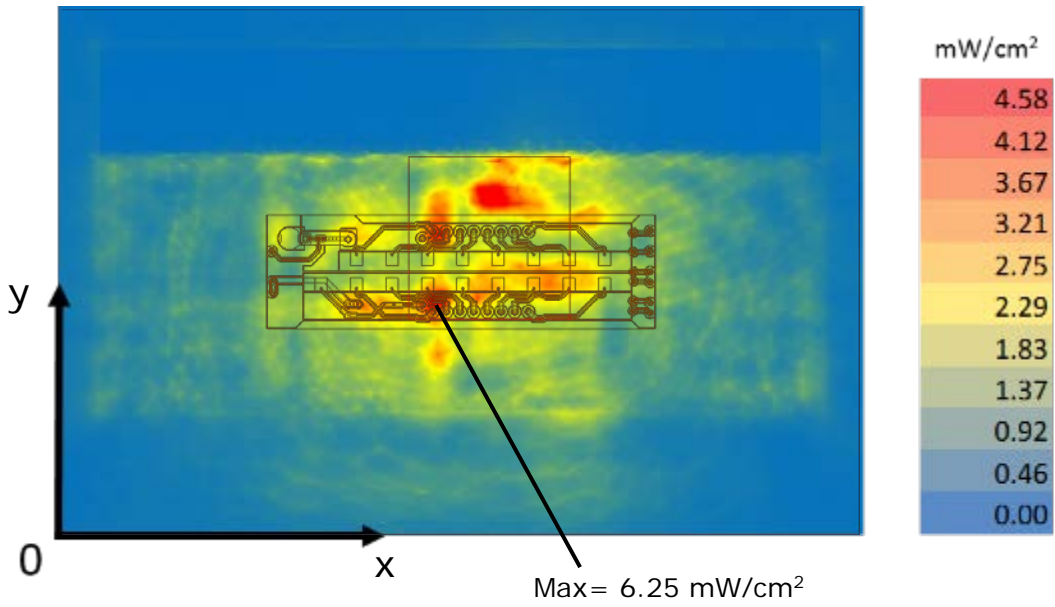


Figure 27 – Channel 3 upper bound, Single-point power density mesh on platform base at 100% duty cycle

4.2.2 Single-point power density values with worst antenna phases for base plane exposure

The Table 6 shows the phase for each antenna elements per channel for the worst case found as described in the chapter 3.4. The phases search algorithm is detailed in point 5 of the section 3.4.3.

Antenna index	Phases [Degrees]		
	Channel 1	Channel 2	Channel 3
0	225	135	315
1	315	270	90
2	45	0	180
3	180	180	0
4	225	270	45
5	315	0	135
6	45	90	225
7	180	180	0
8	0	315	135
9	90	90	270
10	180	180	0
11	0	0	135
12	45	90	270
13	135	180	315
14	225	225	45
15	0	0	135

Table 6 - Phases configurations for the worst case

The amplitude on each antenna is -5.4dBm as explained in chapter 3.7.

Table 7 presents the ratios (linear and logarithmic) at the highest spot value for the Z trajectory on the base area between the power density worst case value along the body direction (S_z) and the power density worst case value along the propagation direction (S_{tot}) for all channels and taking into account all components. This table confirms that the power density component along Z is the principal contributor in the total power density. Also the ratios are used for results scaling in Table 8 of section 4.2.5 and in the compliance summary discussion in Clause 6.

BASE AREA	Channel 1	Channel 2	Channel 3
Mag S_{tot} (maximum poynting spot value with all components) [mW/cm ²]	2.641	4.415	3.083
S_z (trajectory of the above on Z direction) [mW/cm ²]	2.504	3.712	3.028
Ratio (S_z / S_{tot}) (linear)	0.948	0.841	0.982
Ratio $10\log(S_z / S_{tot})$ (dB)	-0.23	-0.75	-0.08

Table 7 – Ratios between Z-power density and total power density on base area

The

Figure

28,

Figure

29

and

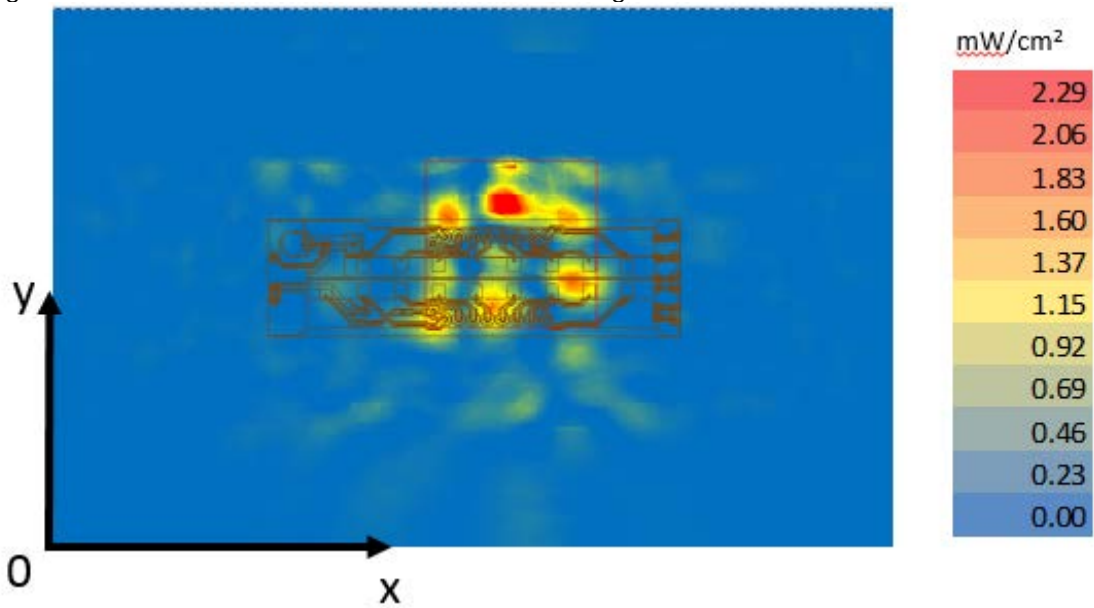


Figure 30 present power density in the body direction using worst case antenna phases presented in the Table 6. The simulated power density area has a size of is 49.5 mm x 32.4 mm, this area corresponds to the blue delimitation.

Worst case coordinates on channel 1 are $x=26.5$ mm, $y= 18.3$ mm.

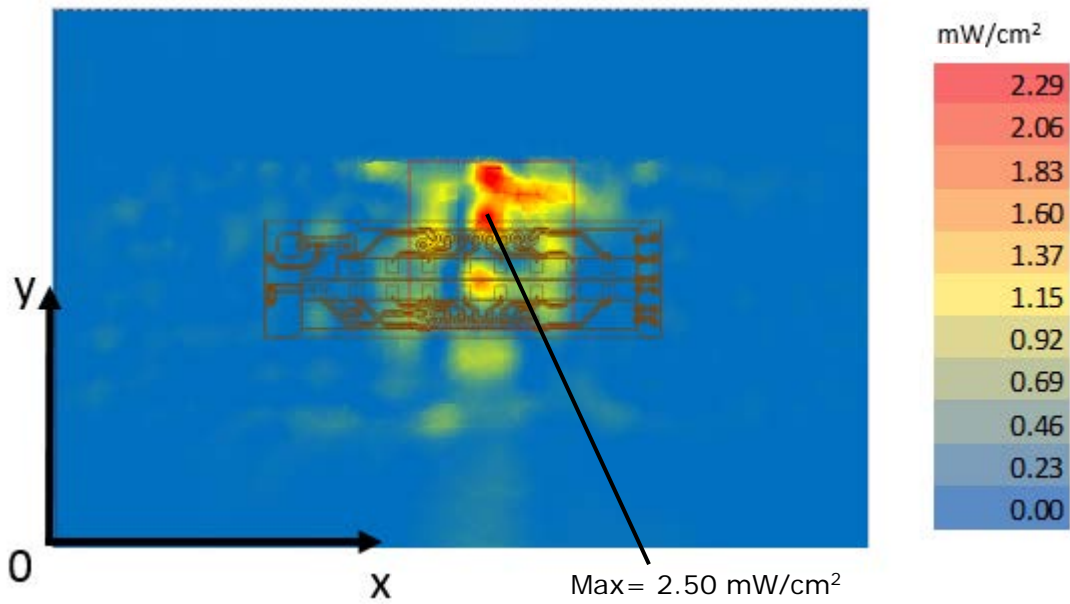


Figure 28 – Channel 1 single-point power density mesh on platform base

Worst case coordinates on channel 2 are $x=26.9$ mm, $y=18.1$ mm

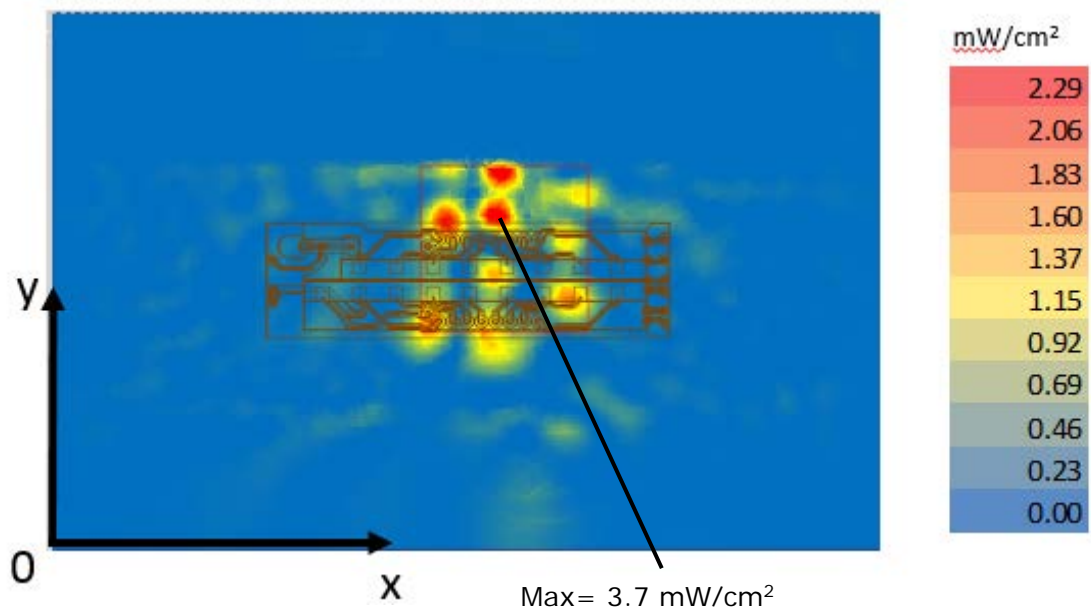


Figure 29 – Channel 2 single-point power density mesh on platform base



Worst case coordinates on channel 3 are $x=26.9$ mm, $y=18.2$ mm

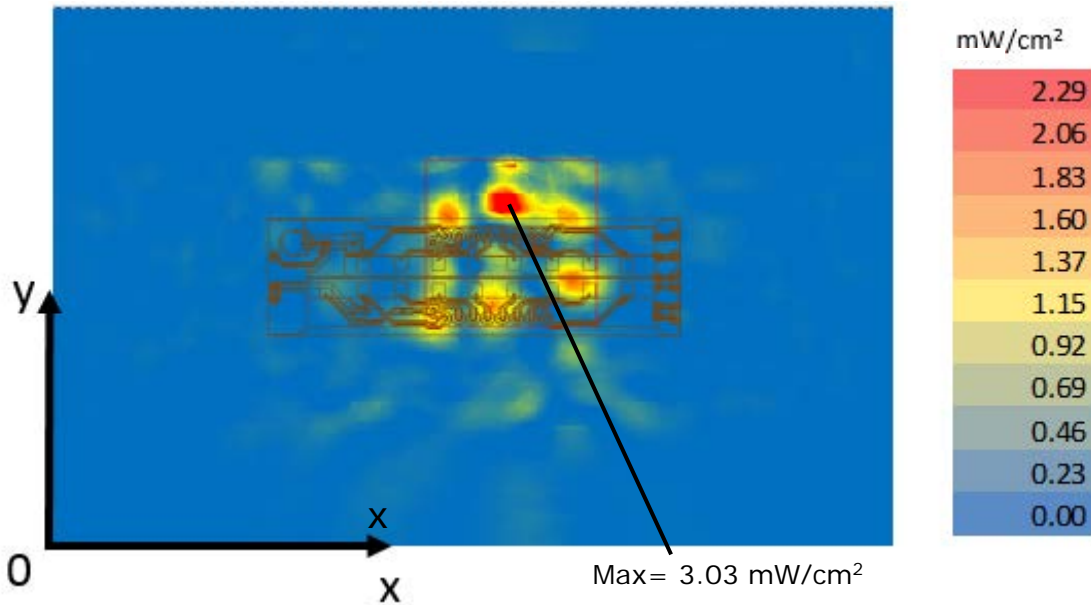


Figure 30 – Channel 3 single-point power density mesh on platform base

The highest value shown in these figures is a point and not yet integrated over the 1cm². The final power density value is given in section 4.2.5.

4.2.3 One dimensional cut of the mesh single-point power density for base plane exposure

In Figure 31 – Figure 33 below, we present a subset of the simulation results from the Z-Single-point power density values with worst antenna phases (chapter 4.2.2).

The subset is a 1 dimensional cut in the X axis and Y axis that shows the behavior of the near field power density at zero distance.

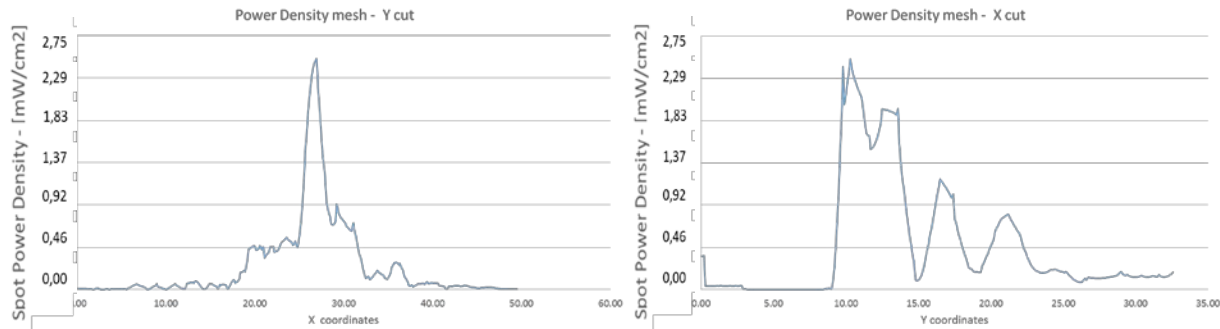


Figure 31 - One dimensional plots of the power density on Channel 1

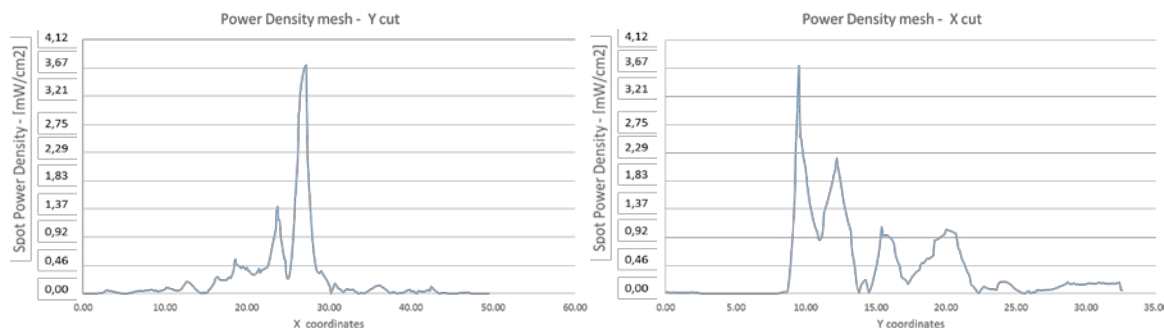


Figure 32 - One dimensional plots of the power density on Channel 2

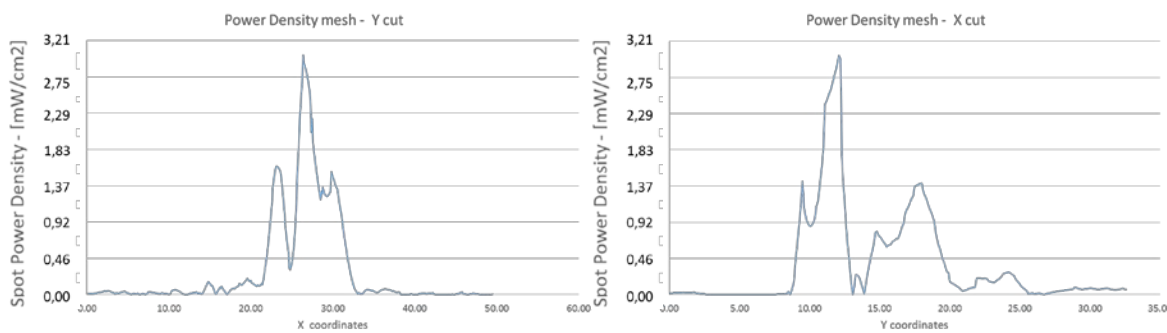


Figure 33 - One dimensional plots of the power density on Channel 3



4.2.4 Integ

Simulation Results

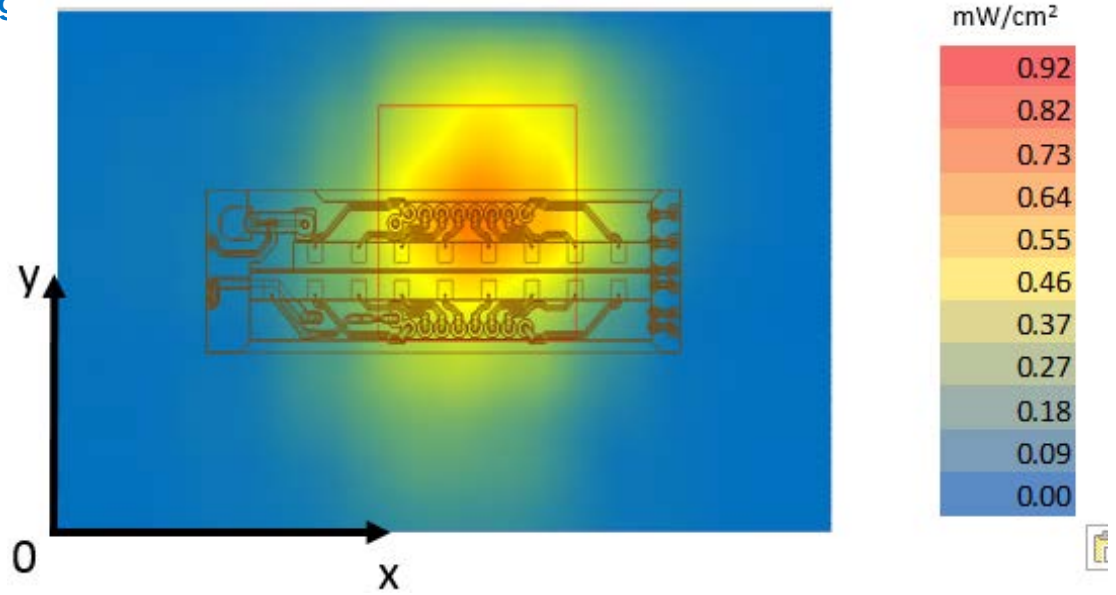


Figure 34 –

Figure 36 below present the Z-integrated power over 1cm^2 at 100% duty cycle for the worst case scenario as explained in section 3.4.3. The plane dimensions of these results is $39.5\text{ mm} \times 22.4\text{ mm}$. The 1cm^2 square location correspondent to the maximum of integrated power density value for each channel is plotted in red in figures below (Figure 30–

Figure 36). The maximum average values are 0.7 mW/cm^2 , 0.64 mW/cm^2 , 0.61 mW/cm^2 for channels 1, 2 and 3 respectively. The worst case coordinates are the center of the squares.

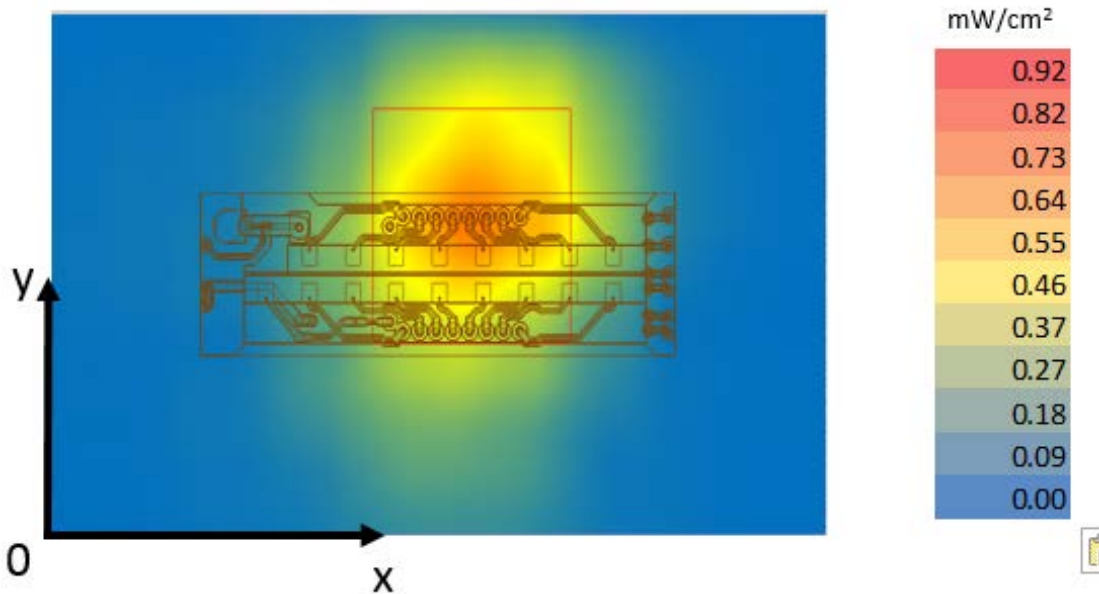


Figure 34 – Channel 1 worst case - Integrated power over 1cm^2 an platform base

Worst case coordinates on channel 2 are $x=21.9\text{ mm}$, $y=13.1\text{ mm}$.

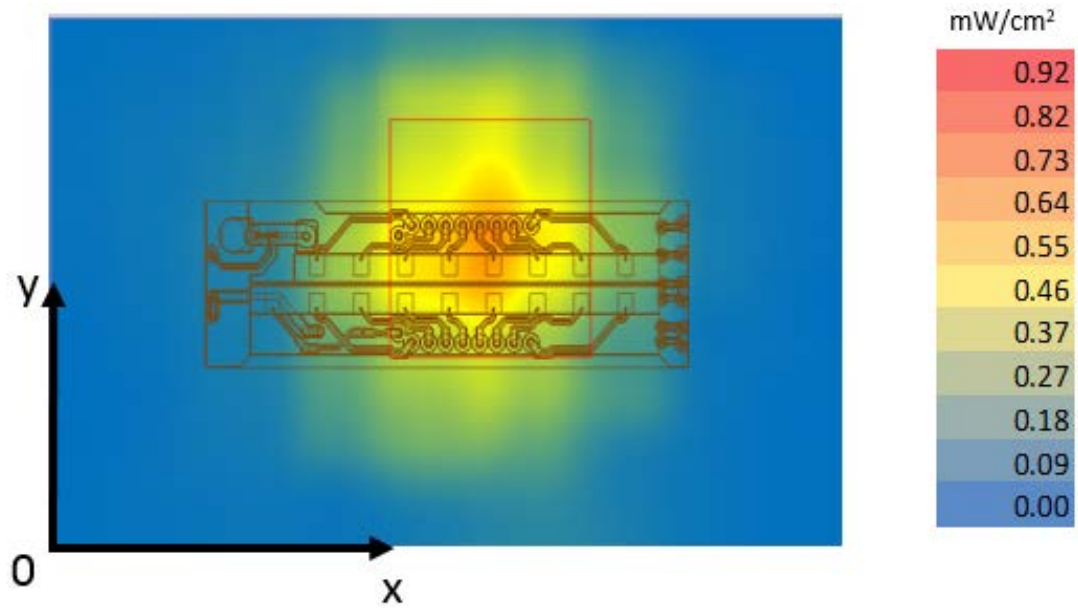


Figure 35 – Channel 2 worst case - Integrated power over 1cm² on a platform base



Simulation Results

Worst case coordinates on channel 3 are $x=21.9$ mm, $y=13.2$ mm.

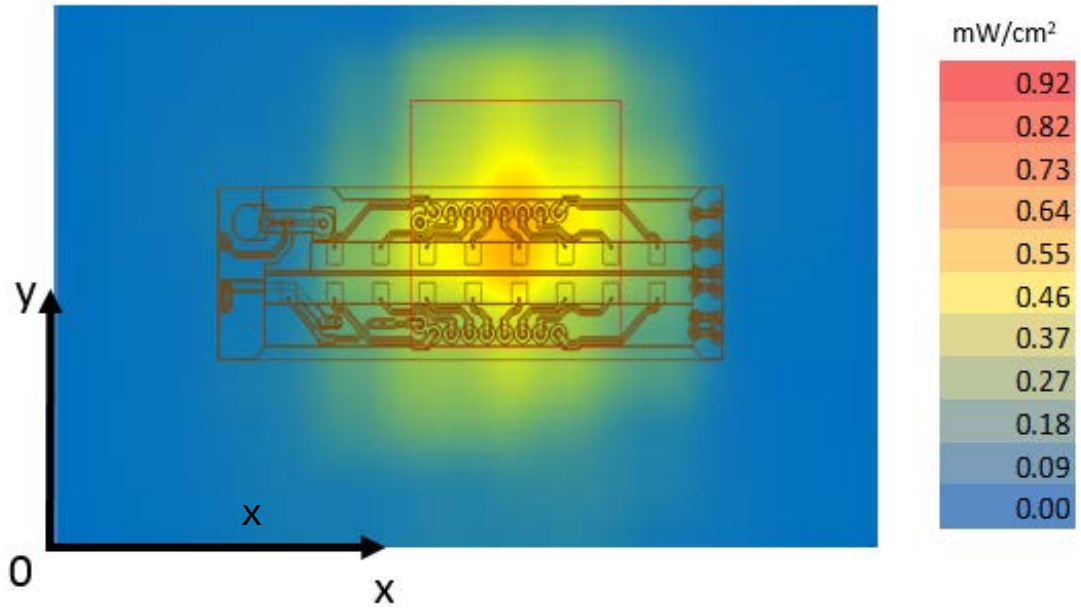


Figure 36 – Channel 3 worst case - Integrated power over 1cm^2 an platform edge



4.2.5 Power density

Figure 37, Figure 38 and Figure 39 show the worst case Z-power-density versus the distance. As described in section 3.4.3 and section 3.6.2 the worst case was computed by the simulation using the worst case antenna phases and the worst platform configuration (Tablet mode). The 0mm reference correspond to the platform boundary, the active antenna located inside the platform is at 14.27 mm from this distance.

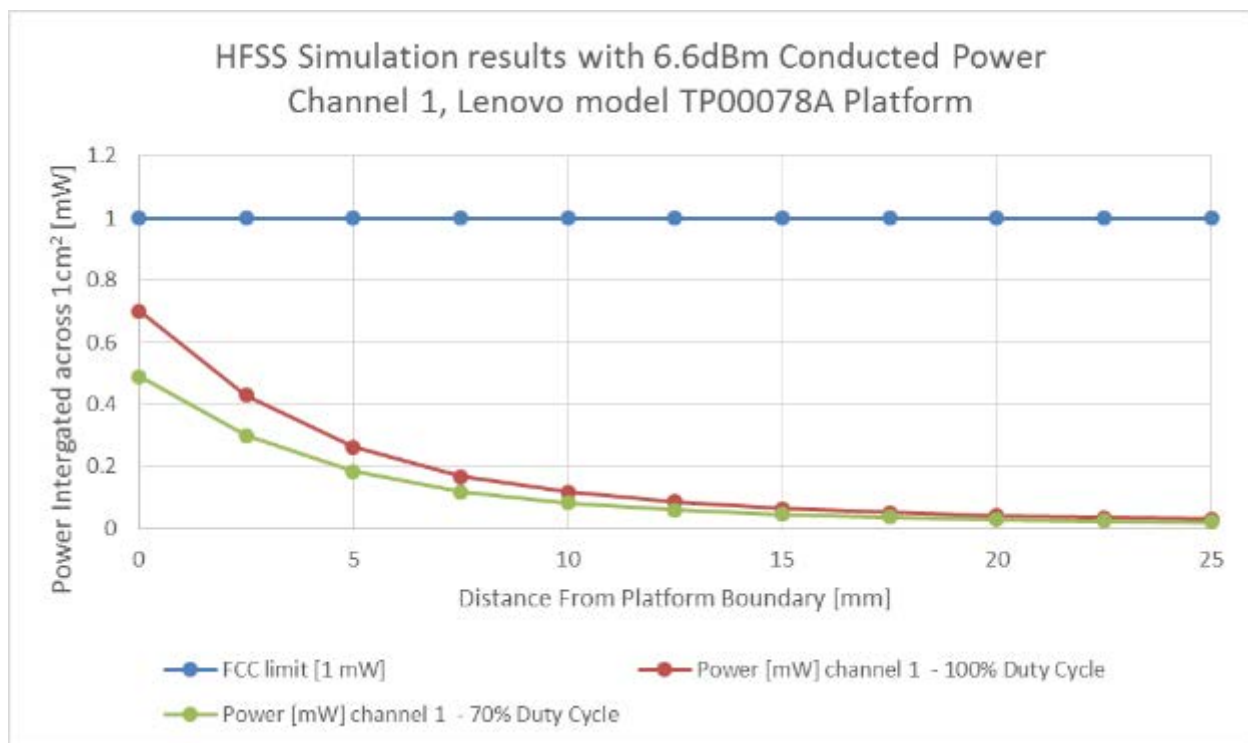


Figure 37 – HFSS simulation results in channel 1

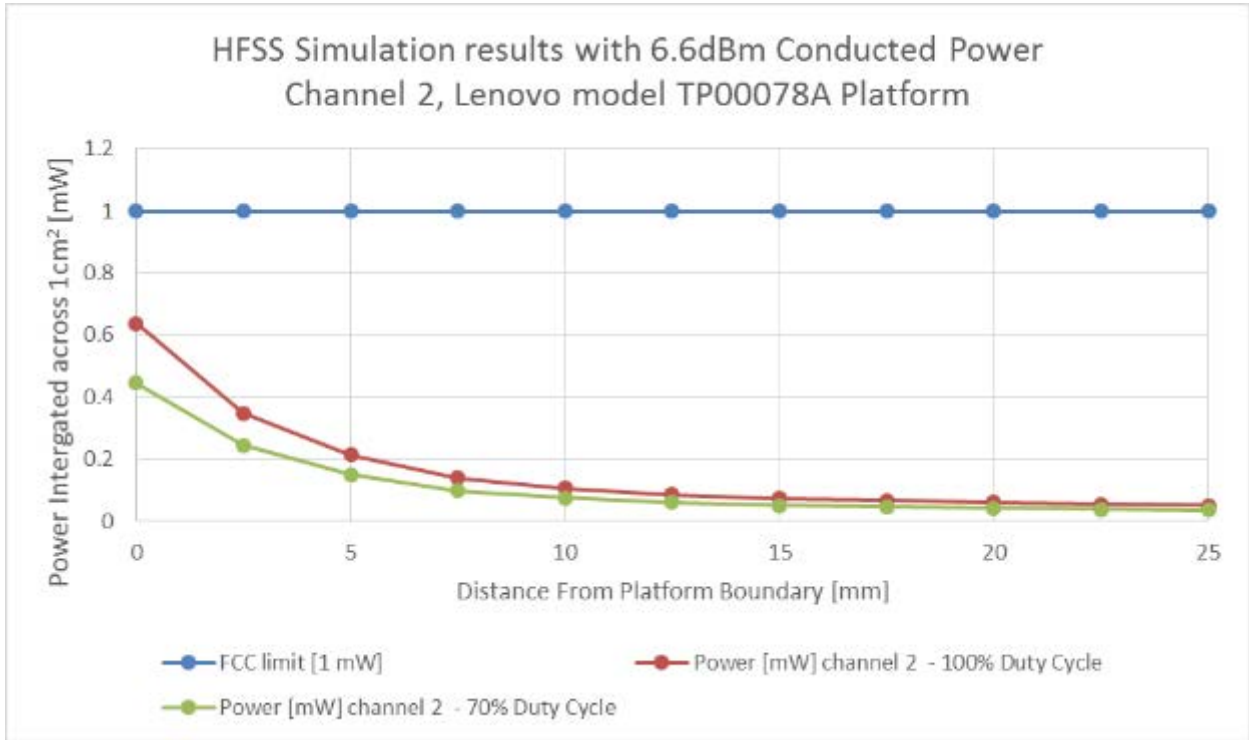


Figure 38 – HFSS Simulation results in Channel 2

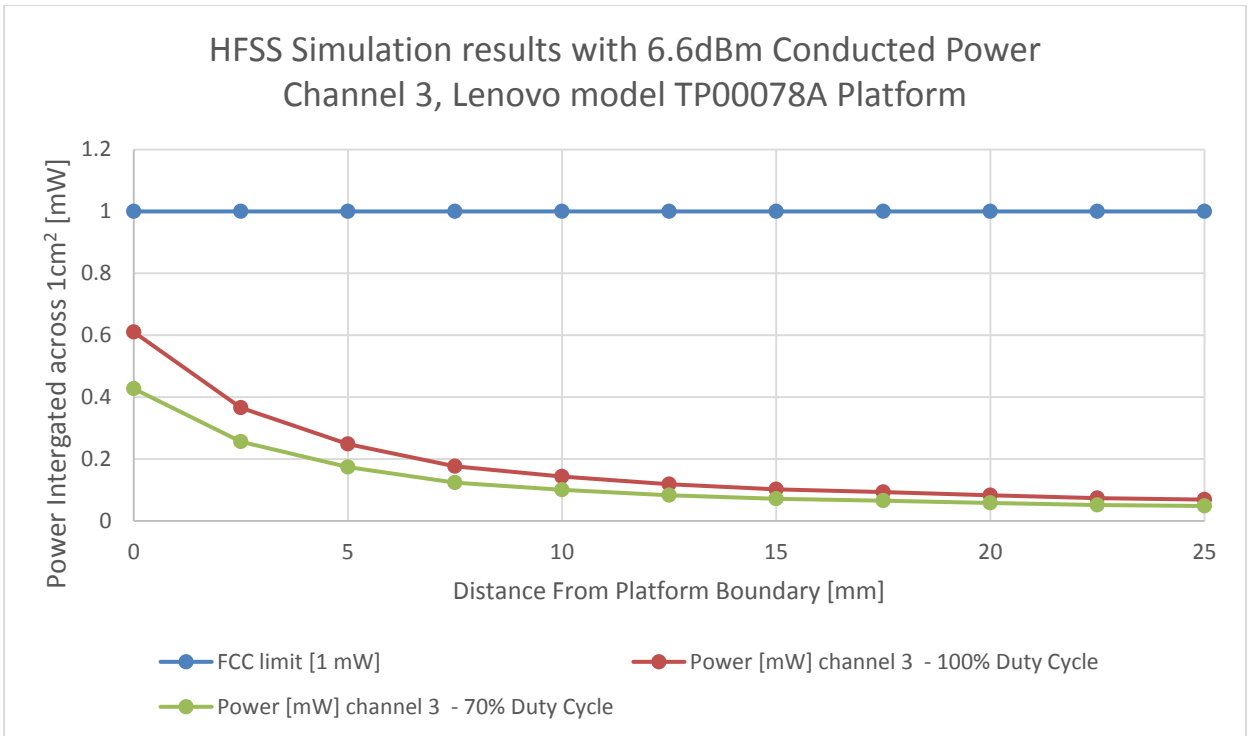


Figure 39 – HFSS Simulation results in Channel 3



Notes for Figure 37 – Figure 39:

1. The worst case channel is channel 1.
2. The Maximum power density (spatially integrated over worst 1cm²) in channel 1 (worst case) is achieved at 0mm distance from the platform boundary and equals to 0.70mW/cm² over 100% duty cycle.
3. As explained in section 2.3, the Intel 18260NGW module is limited to Transmit at a duty cycle of 70% over 10sec. Therefore the maximum spatially integrated and time averaged power density over 1cm² is $0.70 * 0.7 = 0.49\text{mW/cm}^2$.
4. Taking into account the ratios presented in Table 7 between the Z-component and the total power density, the integrated power densities values at zero distances become:

	Channel 1	Channel 2	Channel 3
Integrated Power density in Z-direction <i>(P_z) [mW/cm²]</i>	0.49	0.45	0.43
Corresponding Ratio <i>(R)</i>	0.948	0.841	0.982
Global Integrated Power density <i>(P_{tot}=P_z/R) [mW/cm²]</i>	0.517	0.535	0.438

Table 8 –Base plane integrated power density at zero distance

Therefore, the worst case channel become channel 2 and the maximum spatially integrated and time averaged total power density over 1cm² is $0.45 / 0.841=0.535\text{mW/cm}^2$.

4.3 Conclusion

The simulation results over 2 planes were presented in this report and the simulation on the edge of the platform and the base of the platform are described in the section 3.6.2. The worst case has been shown for the base plane using channel 1 in the Z direction with maximum power density of 0.49mW/cm², and for channel 2 with global components, the maximum power density is 0.535mW/cm². Note that the applicable FCC limit is 1 mW/cm².



5 Validation of Simulation Model in transition-zone Field to Far-Field

Due to the lack of standardized code validation, benchmarking and uncertainty estimations of the simulation software and the implemented device geometry, the near field to far field measurement results are included for the purpose of providing confidence for the software simulation model used and that the results produced were within an acceptable range when compared with the measured results. The error margins of all test results are requested to be considered collectively by the FCC to determine compliance.

To validate the accuracy of the simulation we took a few metrics, presented in this chapter, including correlation of the simulated power density in transition-zone field to far-field against lab measurements. The same simulation was used for both power density estimation in near field (previous chapter) and transition-zone field to far field correlation (this chapter).

5.1 Correlation of power density in far field

Note – the correlation of power density in transition field to far field was done with conducted output power of 3dBm. This value was used for both lab measurements and simulation results.

5.1.1 Far field boundary calculation

Far field boundary can be estimated using *Fraunhofer distance* equation:

$$\text{FarFieldBoundary} = \frac{2d^2}{\lambda}$$

Equation 2 – Far field boundary calculation

In the RFEM 2, d (largest antenna dimension) = 16.1mm (see Figure below)

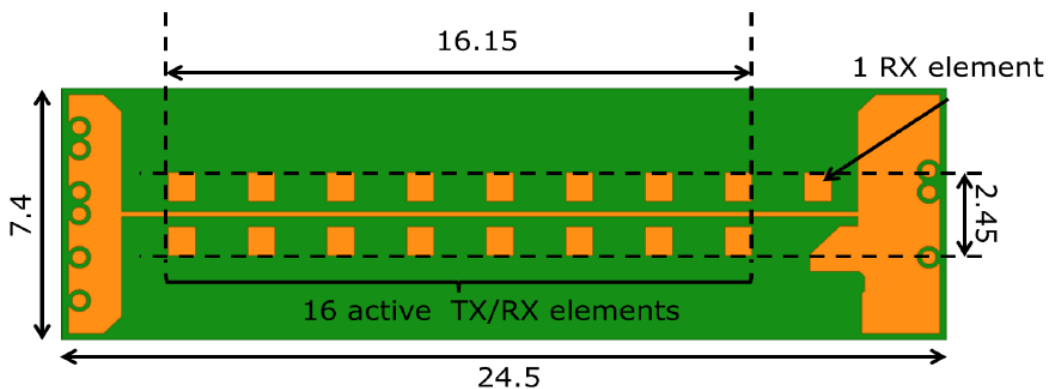


Figure 40 – Antenna Dimensions

Channel	λ (wave length) [mm]	Fraunhofer distance [cm]
1	5.14	10.1
2	4.96	10.5
3	4.79	10.8

5.1.2 Laboratory Test

The measurements were done at the ISO 17025 accredited laboratory Intel Mobile Communications France S.A.S. with FCC registration number #3478.01 on Lenovo Model TP00078A platform with 18260NGW module. Data can be found in lab test report 15110901.TR01, submitted with the application for this FCC ID.

5.1.3 Correlation of measurements and simulation

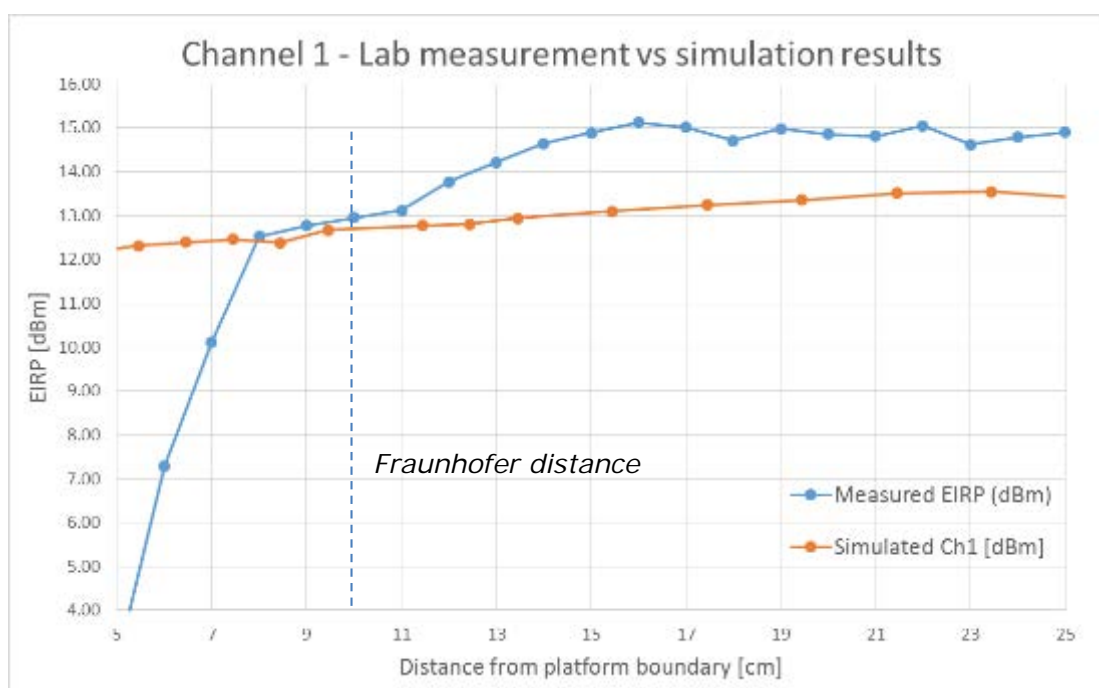


Figure 41 - Comparison of E.I.R.P. simulation results to lab measurements – channel 1



Validation of Simulation Model in transition-zone Field to Far-Field

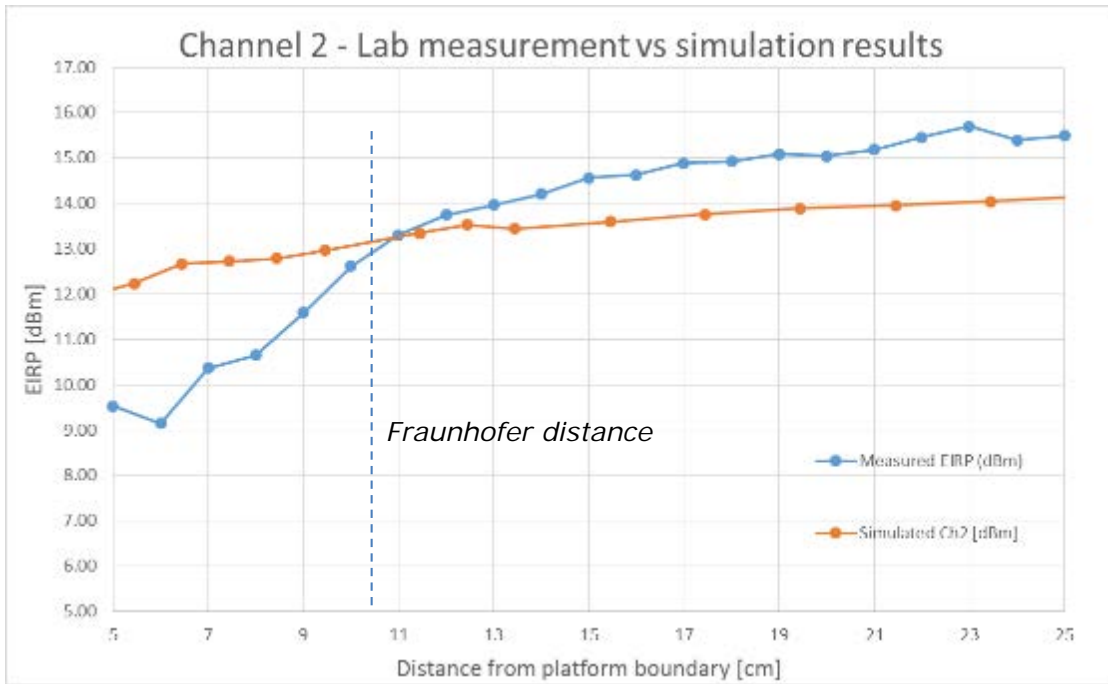


Figure 42 - Comparison of E.I.R.P. simulation results to lab measurements – channel 2

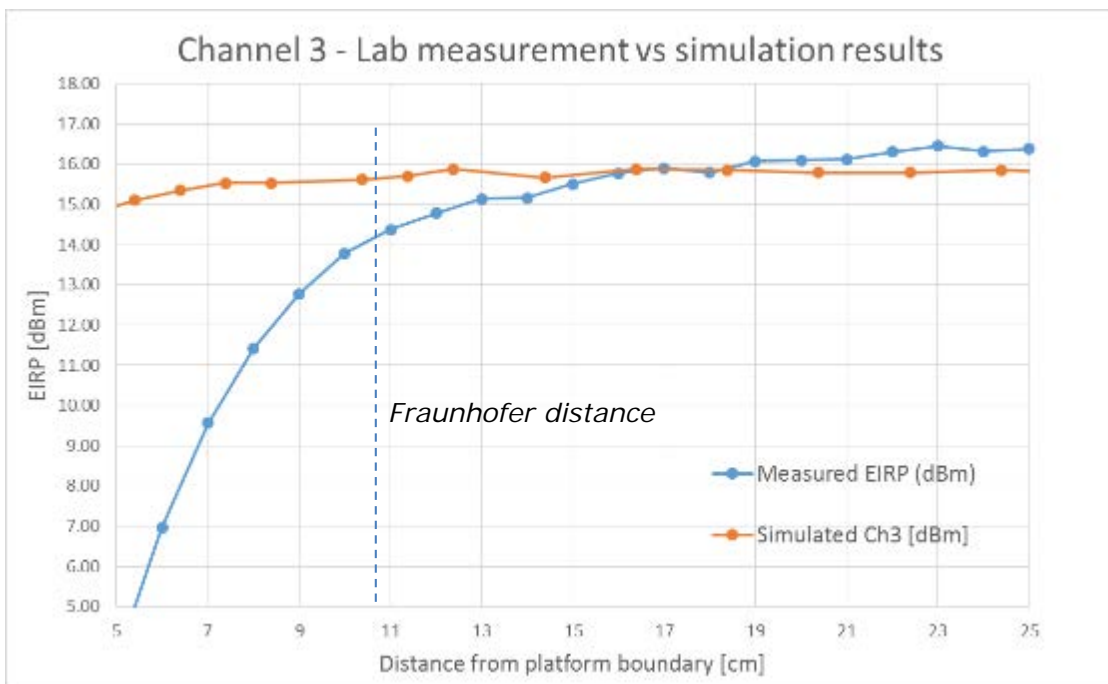


Figure 43 - Comparison of E.I.R.P. simulation results to lab measurements – channel 3



Discussion – correlation results:

The following observations can be made by looking at Figure 41 - Figure 43:

1. Measured EIRP increased to a steady state, demonstrating we are in the transition-zone field below 13-14cm (this is higher than Fraunhofer distance due to the complex platform structure).
2. Good correlation can be seen in steady state power, with up to ~1dB higher measured power than the simulated power.
3. Some difference can be seen in the energy build up between simulation results to lab measurements. This difference is probably due to near field effect and coupling between the platforms to the antenna that is used for the measurements.



5.1.4 Estimating conducted power level

Measured EIRP signal power can be used to estimate the equivalent conducted power that is fed to the antenna array. The estimation is done by subtracting the antenna gain from the estimated EIRP level.

The EIRP level is the same as reported in previous section while the antenna gain is the antenna gain that is used in the RFEM 2 modular approval.

Free space Antenna Gain: Channel 1 – 15.30 dBi, Channel 2 – 15.20 dBi, Channel 3 – 14.8 dBi

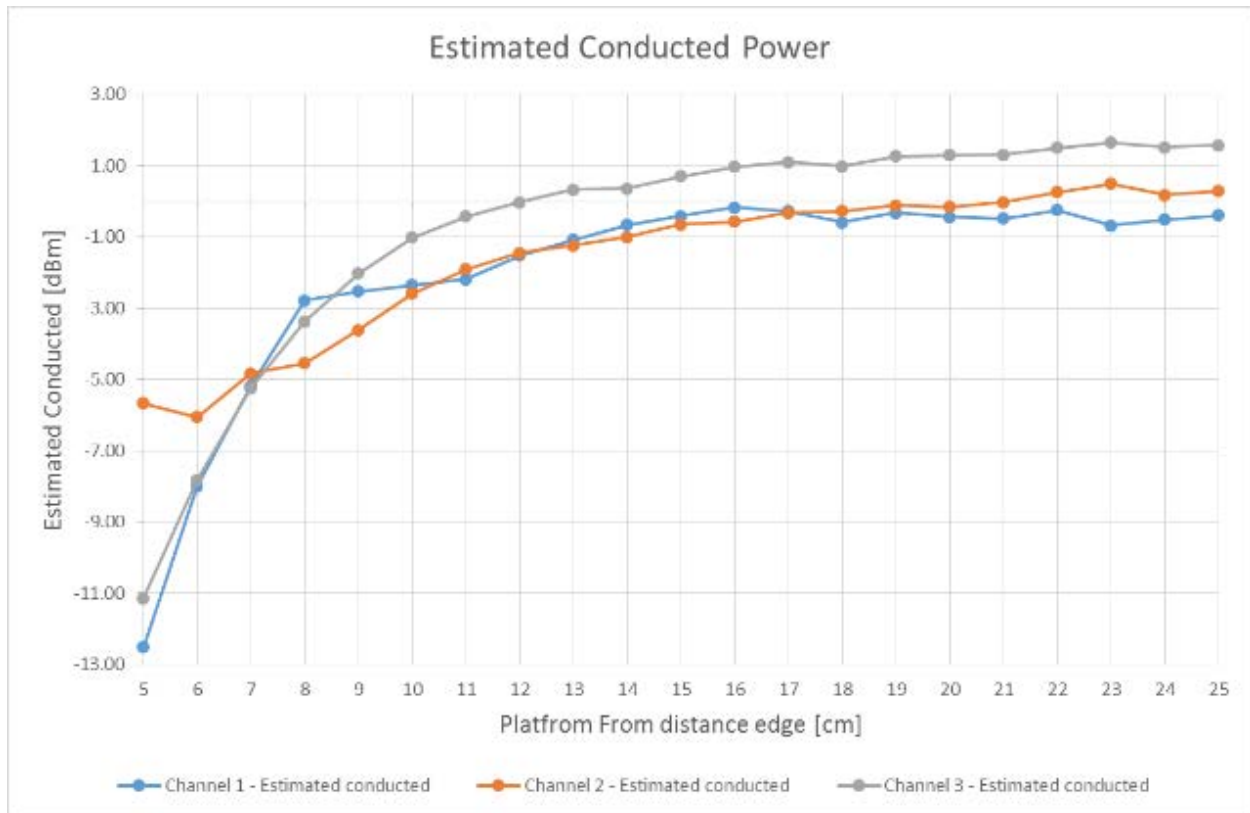


Figure 44 - Estimate conducted power from EIRP data

Discussion – correlation results:

Looking at Figure 44 one can see that the estimated conducted power is lower than the actual power level that was used. The tests were done with a conducted power of 3dBm while the estimated for channels 1 & 2 are ~ 0 dBm & channel 3 ~ 1.5 dBm

1. The antenna gain that is used for this estimation is the modular antenna gain (antenna in free air). However the antenna that is embedded inside a platform has a platform loss that is typically in the vicinity of 1.5 dB~3.0 dB. This additional platform loss explains the estimated power.
2. Lower estimated conducted power can be seen at short distances (up to about 15 cm) as coupling with the measuring device or other near objects. In addition at this range (4-10 cm) the antenna gain is lower than the far field antenna gain, hence EIRP is lower and the predicted power is lower.

5.2 Simulating a canonical antenna design

A simple patch antenna with Length = 7.5 mm (GND plane length), and Lambda = 4.8 mm, and was designed to work at 62.5GHz, as can be seen in the figure below.

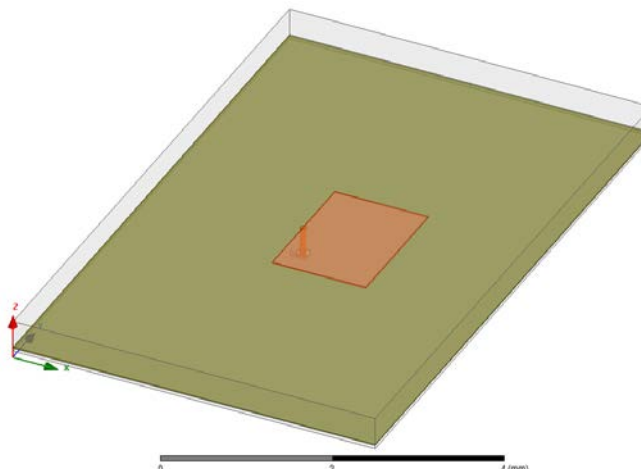


Figure 45 - Simulation of a single Patch antenna

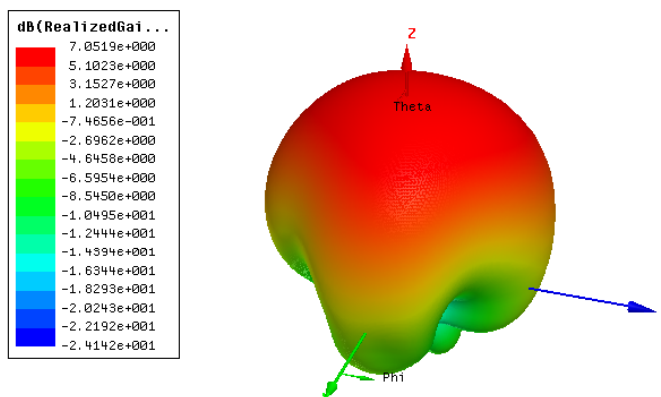


Figure 46 – Patch Antenna Gain

The simulated Far-Field Max Realized Gain [dBi] is 7.05[dBi], as simulated by far field simulation. The 7.05 dBi gain was obtained using HFSS simulation using Far Field Gain option.

Theoretically patch antenna gives ~7-9 dBi gain. The simulated patch antenna in the HFSS simulation is not a theoretical patch, it includes several "real life" non-idealities (width, size, feeding point etc). The 7.05 dBi Max Realized Gain is the gain obtained from HFSS simulation including those non-idealities.

A few test planes were integrated into the simulation at different far-field distances from the patch (shown below) for power density calculations:

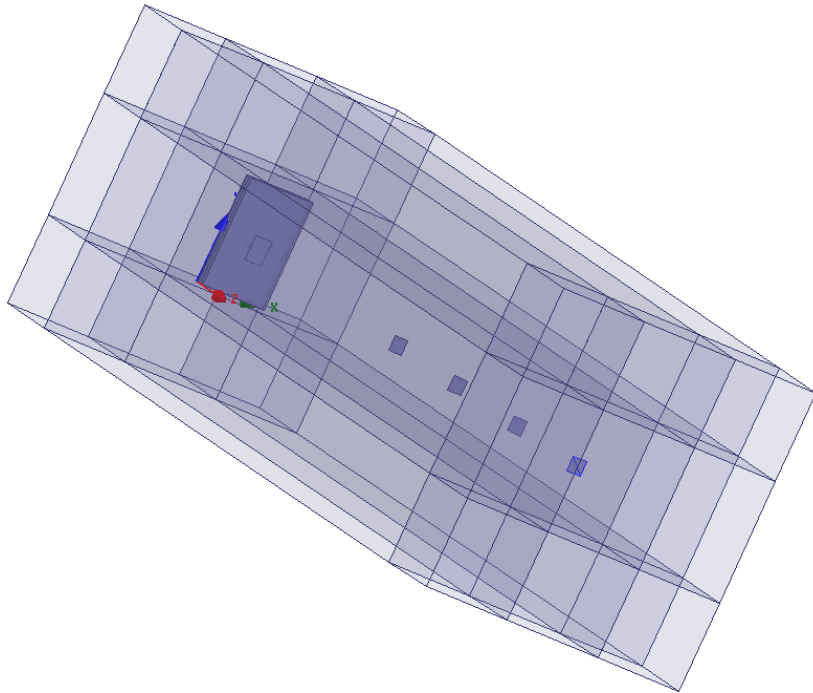


Figure 47 – Simulation 3D structure

The distances between the patch and the test planes range from 24mm to 54mm.

To validate the numerical tool, the power density results at the test planes are translated into gain using omnidirectional power propagation and compared to far field gain according to simulation (table below).

The table below summarizes the results:

Far Field Distance	$P_{omni} = \frac{P}{4\pi R^2} \left[\frac{W}{mm^2} \right]$	Power Density from simulation $\left[\frac{W}{mm^2} \right]$	Gain calculation from power density [dBi]
24mm	1.34e-4	6.70e-4	6.99
29mm	9.11e-5	4.61e-4	7.04
34mm	6.59e-5	3.38e-4	7.10
44mm	3.91e-5	2.03e-4	7.15
54mm	2.59e-5	1.35e-4	7.17

Table 9 – Gain calculation from power density per several distances

Where P is the simulated radiated power and R is the distance from the patch to the test plane.

The table above shows excellent correlation between the Patch antenna gain calculated from power density, to the Far-Field Max realized gain (7.05[dBi]). This is also depicted in the figure below:

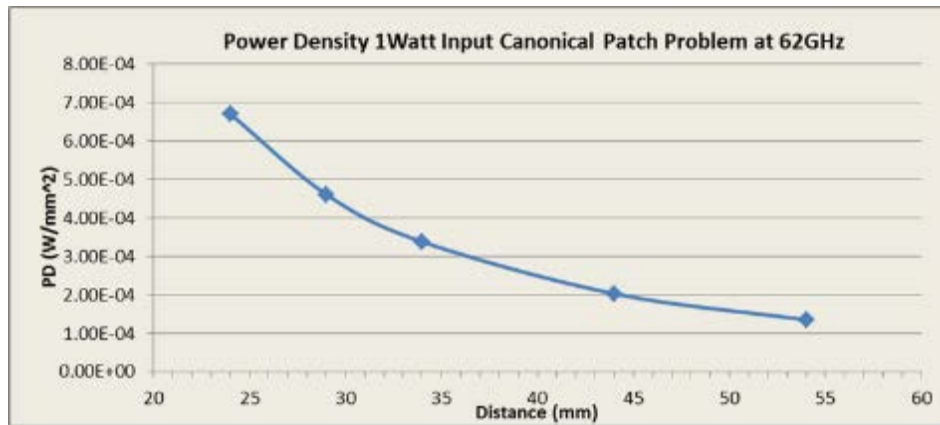


Figure 48– Power density of canonical patch antenna



6 Summary

Due to the lack of standardized code validation, benchmarking and uncertainty of the simulation software, the near field to far field results are included for the purpose of providing confidence for the software simulation model used and that the results produced were within an acceptable range when compared with the measured results. The error margins of all test results are requested to be considered collectively by the FCC to establish confidence for the accuracy of the HFSS simulation.

Per consultation with FCC staff, it is accepted to use the adjustment of power density based on differences between the normal component of the Poynting vector and total field using the simulation results for the worst case antenna configurations for this specific filing and circumstances only.

The following table summarizes the simulation results in the near field of Intel 18260NGW module, embedded in Lenovo Model TP00078A:

Parameter	Value
Total conducted power	6.6 dBm
Maximum TX duty-cycle	70%
Maximum spatially integrated and timed average power density, over 1cm ² and 10 seconds (CH1)	0.49 mW/cm ² (FCC Limit : 1 mW/cm ²)
Maximum spatially integrated and timed average power density, over 1cm ² and 10 seconds taking into account the ratios presented in Table 7 (CH2)	0.535 mW/cm ² (FCC Limit : 1 mW/cm ²)

Table 10 – Summary of simulation results for RF exposure compliance

Therefore Intel 18260NGW module, embedded in Lenovo Model TP00078A, complies with FCC rule parts §2.1093 and §15.255(g).